1

Patch ClampTechnique for Looking at Serotonin Receptors in B103 Cell Lines: A Black Box Test

K. Fatima-Shad[1] and K. Bradley[2]
[1]*PAP RSB Institute of Health Sciences, Universiti Brunei Darussalam*
[2]*Faculty of Medicine and Health Sciences, University of Newcastle*
[1]*Brunei Darussalam*
[2]*Australia*

1. Introduction

In this chapter, we would like to describe black box testing phenomenon of patch clamp technique while looking at the serotonin receptors in B103 cell lines.

In a black box test, the tester only knows the inputs and what the expected outcomes should be and but not the mechanisms of those outputs. Patch clamp method is a great method for quantifying the research on Pico or femto scales, but most of the time even very controlled experiments will not give us the expected results. We will begin our chapter by introducing serotonin receptors and B103 cell lines.

In mammals, serotonin or 5-hydroxytryptamine (5-HT) behaves primarily as an inhibitory neurotransmitter of the central nervous system (CNS), decreasing neuronal activity and facilitating behavioural relaxation, while peripherally it has an excitatory role, promoting inflammatory responses, pain, and muscle spasm (Kirk et al 1997). Centrally this neurotransmitter is produced nearly exclusively by a group of neurons found in the rostro-ventral brainstem comprising the raphé nuclei from which project two major serotonergic pathways (Dahlstrom & Fuxe, 1960).

There are more than seventeen types of serotonin receptors and almost all are associated with G-proteins except 5-HT_3R, which is a member of the ligand-gated ion channel superfamily. The 5-HT_3R was initially identified as a monovalent cation channel by studies indicating that extra-cellularly recorded depolarising responses were diminished by removal of Na^+ from extracellular solution (Wallis & Woodward, 1975). The native 5-HT_3R is a cation-specific ion channel, but is otherwise relatively non-selective (demonstrating poor cation discrimination) allowing the passage of even large molecules, such as Ca^{2+} and Mg^{2+} (Maricq et al., 1991).

Serotonin type 3 receptors have been identified in the enteric nervous system (Branchek, et al, 1984), on sympathetic, parasympathetic, and sensory nerve fibres in the CNS (Kilpatrick et al, 1987), and on several mouse neuroblastoma cell lines, including the NCB-20 (Lambert et al., 1989, Maricq et al., 1991), N1E-115 (Lambert et al., 1989), and NG 108-15 (Freschi & Shain, 1982). All of these lines exhibits a rapid membrane depolarisation accompanied by increased membrane conductance in response to exogenously applied 5-HT (Peters & Lambert, 1989).

We are using B103 cell lines to study this fast acting receptor channel. The B103 rat neuroblastoma cell line was produced via transplacental exposure to nitroethylurea (Druckrey et al., 1967) and literature (Tyndale et al., 1994; Kasckow, et al., 1992) indicated the possibility that this line could be derived from cells of the raphé nuclei, and so might be representative of cells from the serotonergic pathway. The B103-line has been used as a model in a number of studies looking at GABA function, including GABA uptake (Schubert, 1975), and binding (Napias, et al., 1980). Studies looking at the functionality of $GABA_A$Rs in a number of the lines initially generated (Schubert et al.,1974) via the patch-clamp technique indicated that while all lines were suitable for patch-clamp studies, none showed appreciable $GABA_A$-induced chloride conductance. Although the B103-line was not used in this study, it was reasonable to assume that it might exhibit similar characteristics and be suitable for electrophysiological studies (Hales & Tyndale, 1994). This was supported by the findings of (Kasckow et al., 1992) where patch clamping detected no functional $GABA_A$ chloride channels in the B103-line. Other studies involving the B103-line have centred around exploring the characteristics of Alzheimer's disease (specifically neuritic plaques) with particular focus paid to the β-amyloid peptide (Mook-Jung, 1997), and β/A4 protein precursor (Ninomiya et al, 1994).

Membrane excitability of the line was initially confirmed using anode-break stimulus, while ^{125}I-α-neurotoxin binding indicated the presence of AChRs. B103 cells were shown to contain the neurotransmitter GABA, and both choline acetyl transferase and glutamic acid decarboxylase activities – enzymes acting in ACh and glutamate anabolism (Schubert et al., 1974). This cell line has also been used for looking at the effects of extracellular Ca2+ influx on endothelin-1-induced mitogenesis, as B103 neuroblastoma cells predominantly express endothelin ETB receptors (Yoshifumi et al, 2001)

It has been shown previously that metastatic cells express high levels of voltage-gated Na+ channels (VGSCs) in prostate cancer (Laniado et al., 1997), breast cancer (Fraser et al., 2002; Roger, et al., 2003) and melanoma (Alien, et al, 1997).

Although, the cell line has previously proven suitable for patch clamp study, no work had yet been conducted about the presence of serotonin type 3 receptor channels and their relationship with the types of VGSCs for these cells.

The patch clamp technique has been applied to the B103 cell line in this experimental series in order to explore the native voltage-gated channels (VGCs) and serotonin sensitivity to type 3 receptors present in these cells. This project is aimed to explore whether these cells presented active/functional serotonin type 3 receptors (5-HT_3R) and voltage-gated sodium channels (VGSCs) and the link between each other.

2. Experimental procedures and methods

2.1 Cell culture

The B103 cells were donated by Dr Phil Rob (Cell Signalling Unit, Westmead). Stock aliquots were stored at -80°C and active stocks used for 20-25 passages before a new aliquot was revived – passage limitation decreased the incidence of cellular mutation (Figure 1).

Twice a week confluent active stocks were split and new flasks seeded in neuronal growth medium (NGM) (DMEM (TRACE), 10% foetal calf serum (FCS), 2% of 7.5% sodium

bicarbonate, 200 mM L-glutamine, 2% 1 M HEPES). Five minute incubation in trypsin at 37°C, 5% CO_2, 90% humidity (Forma Scientific incubator) degraded the extra cellular matrix of the culture, releasing cells from flask adhesion (effective dislodging turned the trypsin cloudy).

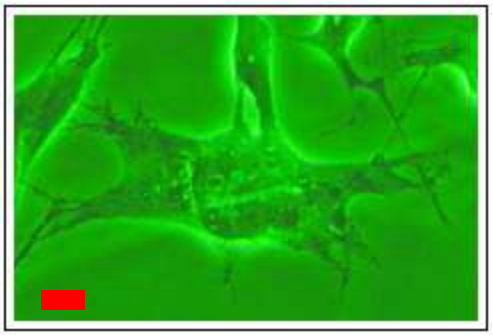

Fig. 1. A Sample Mutated Cell from the B103 Clonal-Line. Taken with an Olympus inverted microscope at 30× magnification showing dramatically altered morphology. These cells were typically seen to engulfing neighbouring cells.

Trypsin was inactivated by adding NGM, preventing continued digestion, which would have resulted in cell lysis. The suspension was spun at 400 rpm for 8-10 minutes in a megafuge (Heraeus Instruments). Supernatant was discarded and cell pellet gently resuspended in 10 ml NGM.

Later on cells were replated (Figure 2) and cover slips were prepared for patch clamp experiments.

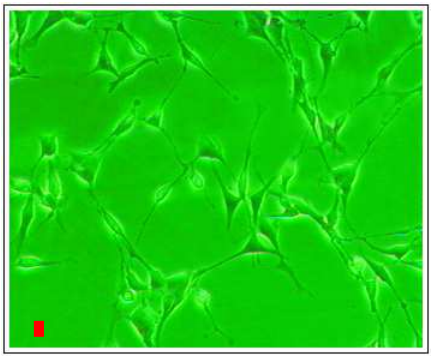

Fig. 2. A Typical B103 Cell Culture. Image at 10× magnification after 48 hours of incubation, showing a cellular concentration of 4.0×10^5. Note the extensive branching network generated.

2.1.1 Cell counting

Cells were counted from the outer four segments of a **hemocytometer** (Improve Neubave Weber) under **10×** magnification (using an Olympus CK2 microscope) and a total mean

value was calculated. This value was used to determine the concentration of cells per millilitre in the diluted cell suspension by employing the formula:

mean cell count × 100 000 (gave a per ml value) = cells/ml

After cell concentration was calculated, the cell suspension was diluted to **1.0×10^5 cells/ml** and the cells plated at varying concentrations onto sterilised collagen-coated coverslips (see heading Collagen-Coating the Coverslips) in **35 × 10 mm tissue culture dishes** (Corning). The cellular concentration required for later work was **4.0×10^5** and because cells roughly **doubled** every **24 hours**, plates were seeded with four different cellular concentrations (Table#1).

Day of Use	Plating Cell Concentrations	Cell Culturing	
		FCS Media (ml)	Cell Suspension (ml)
Day 1	seeding performed	-	-
Day 2	2.0×10^5*	0	2
Day 3	1.0×10^5*	1	1
Day 4	5.0×10^4*	1.5	0.5
Day 5	2.5×10^4*	1.75	0.25

* Because of the doubling rate of neuronal cells, plates reached a concentration of 4.0×10^5 on their respective days of use.

Table 1. Cell Culturing Schedule

2.1.2 Collagen-coating the coverslips

Collagen provided a matrix for B103 cell adhesion when plated. Coverslips and culture dishes were coated with sterile **10 μg/ml** rat tail **collagen solution** (Roche) diluted in **phosphate buffered saline** (PBS), and incubated at **37°C** for **2 hours**. The collagen solution was removed and dishes washed with PBS to ensure complete removal of residual collagen.

2.2 Solutions

Cells were patched under two different sets of bath and pipette solutions. Initial results were obtained from physiologically normal solutions (normal pipette solution: 120 mM KCl, 3.7 mM NaCl, 1 mM $CaCl_2$, 2 mM $MgCl_2$, 20 mM TEACl, 10 mM HEPES, 11 mM EGTA (pH 7.4); normal bath solution: 137 mM NaCl, 5.4 mM KCl, 1.8 mM $CaCl_2$, 2 mM $MgCl_2$, 5 mM HEPES, 10 mM D-glucose (pH 7.4)) which were designed to mimic normal cellular conditions. Later recordings utilised solutions with symmetrical cation concentrations (normal pipette solution: 140 mM NaF, 1 mM $MgCl_2$, 10 mM HEPES, 10 mM EGTA (pH 7.4); experimental bath solution: 140 mM NaCl, 2 mM $CaCl_2$, 1 mM $MgCl_2$, 10 mM HEPES, 10mM

D-glucose (pH 7.4)). To promote long-term cell viability bath solution osmolarity was kept between 300-320 mOsm. A difference of 20 mOsm rendered cells non-viable for electrophysiological study (adversely affecting plasma membrane structure and function) either resulting in cell swelling (<300 mOsm) or shrinking (>320 mOsm) leading to premature cell death. The bath perfusion system was used to elute the cell cultures and was comprised of a solution reservoir connected to the bath via plastic tubing. A regulator was attached to the tubing allowing for control of solution flow – unrestricted flow was 0.38 ± 0.009 ml/sec.

2.2.1 Bath solution perfusion

Solution was removed from the bath and emptied into a waste reservoir via a system of tubing connected to a **miniport motor** (Neuberger). Between the waste reservoir and the motor was a second reservoir containing **silica gel crystals** which prevented moisture from reaching the motor.

The bath perfusion system was particularly prone to contamination, especially with bacteria which fed on the solution glucose. To prevent contamination the system was rinsed with distilled water after every use to remove any trace glucose. However when the inevitable contamination did occur **antibacterial solution** (Milton hospital-grade disinfectant) was used to flush the lines.

2.2.2 Technical difficulties

The technique employed for electrophysiological study of the B103 cell-line was not conducted under aseptic conditions therefore the cells were particularly prone to **bacterial infection**. Bacteria tended to attack the cellular **cytoplasm** forming small **vacuoles** (Figure#3) and rendering the cells unfit for study. Once an infection had been noted, in order to prevent further contamination (particularly of the surrounding equipment) the patch-clamp system had to be immediately decontaminated using **70% ethanol** and/or **antibacterial solution**. The coverslip had to be immediately discarded and the stage and bath had to be thoroughly disinfected to prevent contamination of subsequent coverslips.

2.3 Pharmacological agents

The following pharmacological agents were used: Serotonin, Ondansetron, Tetrodotoxin (TTX), Phenytoin, and d- Tubocurarine. All these were purchased from Sigma, except TTX (Alomone).

2.4 Patch clamp experiments

Cells were visualised with an Olympus IX70 inverted microscope and images recorded with a KOBI digital colour camera and the ASUS Live 3D Multimedia software. Electrophysiological manipulation and recordings were undertaken with a HEKA EPC9 amplifier and HEKA *Pulse* software package which supersedes older amplifier models by having a fully interactive, PC-compatible data retrieval and storage facility. The *PULSE* program allowed for automatic electronic noise adjustments such as fast and slow capacitative transients' nullifications.

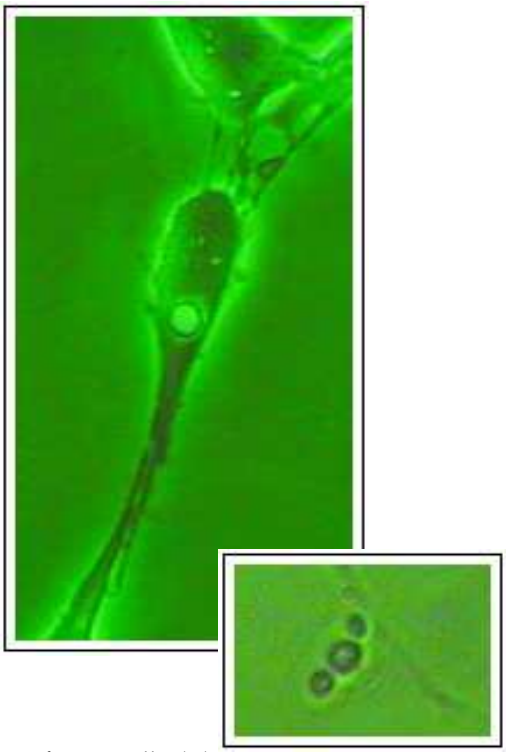

Fig. 3. Bacterial Infection of B103 Cells. **(A) Cytoplasmic Vacuole.** Bacteria entered the cells by generating holes in the cell membranes where they formed vacuoles in the cytoplasm. Image generated under phase-contrast filtering at 30× magnification. **(B) Bacterial Aggregate.** Image generated at magnification under bright-phase filtering at 60× magnification.

Thin walled borosilicate glass capillaries (1.5 mm O.D. × 1.17 mm I.D) were used to produce patch pipettes with a 3 MΩ resistance. Pipettes were half-filled using both the front- and back-filling techniques. Solution-filled glass pipettes were attached to an Ag/AgCl recording electrode and manipulated using a PCS-5000 series patch clamp micromanipulator (Burleigh Instruments). Cellular patching was performed according to the protocol outlined by (Hamil et al., 1981) Figure 4.

An appropriate B103 cell was chosen for patching on the basis of its general morphology: approximately 25 μm in diameter, well-defined clean cell membrane, and relatively isolated from contact with other cells. Morphological cellular standardisation was a critical component of the protocol. All cells were tested for their viability in the physiological saline before changing into symmetrical solutions (sodium on both side of the cell membrane) for measuring voltage activated sodium currents. 5-HT3 receptor channel currents were observed in B103 cells, when they were exposed to serotonin (endogenous currents of B103 cells were completely abolished by using TTX or Phenytoin).

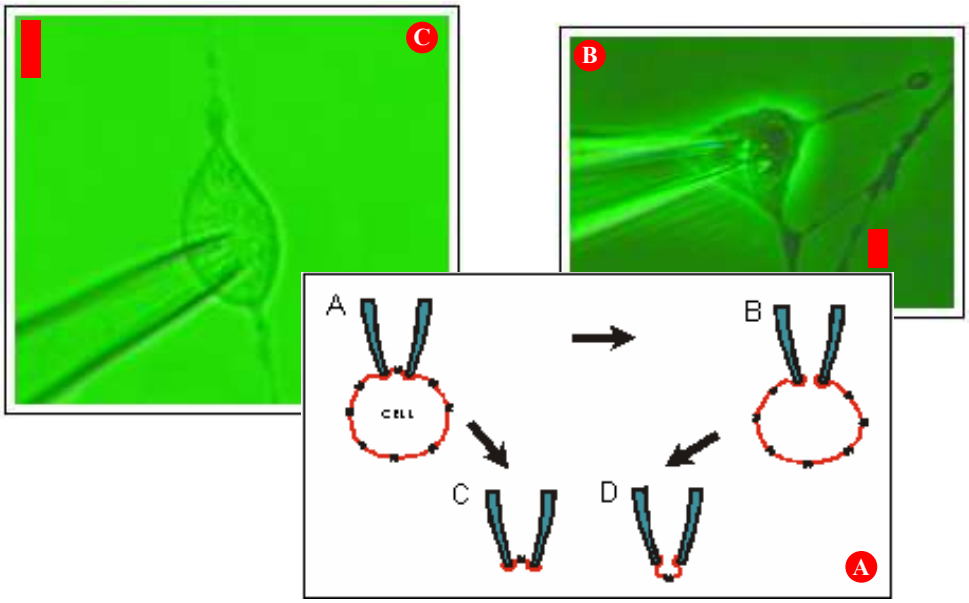

Fig. 4. (A) The Various Patch-Clamp Configurations. A indicates the cell-attached configuration where a pipette is attached to the outside of a cell with a GΩ resistance and effectively measures the conductance of a single channel. B shows the whole-cell patch-clamp configuration where the patch of membrane under the pipette tip has been ruptured allowing direct access to the cell interior so that pipette solution replaces the cytoplasmic contents of the cell. This configuration forms a continuous circuit with the electrode and the cell interior allowing for recordings of the conductance of channels from the entire membrane. Both of these configurations were used during this experimental series, while C (the inside-out) and D (outside-out) configurations were not used. **(B) A Cell-Attached Patched B103 Cell under Phase Contrast Filtering**. At 40× magnification **(C) A Whole-Cell Patched B103 Cell under Bright Phase Filtering**. At 30× magnification. Immediately after patch initiation cell will start to take on a slight spherical appearance.

A perfusion system was employed to introduce chemicals (both agonist and antagonist) onto a patched cell with application time being electronically controlled via solenoid valve. The agonist solutions used in this experimental series were a set of serotonin hydrochloride dilutions: 1 mM, 500 μM, and 10 μM. Patched cells were challenged with a 8000 ms exposure to agonist at 5 minute intervals – a transient method of agonist application avoided cellular desensitisation (Neijt et al., 1988), and results were recorded using the HEKA *PULSE* software. The solution used in our experiments to abolish serotonin activated current was Ondansetron a selective 5-HT3R antagonist. Cells were again challenged with 8000 ms exposure, both with and without agonist or antagonist solution.

Cells were stimulated using a Pulse Protocol facilitated via the HEKA *Pulse* software. Cellular stimulation ranged from -100 mV to +30 mV increasing in 10 mV steps with a resting period at 0 mV between each step (figure 5)

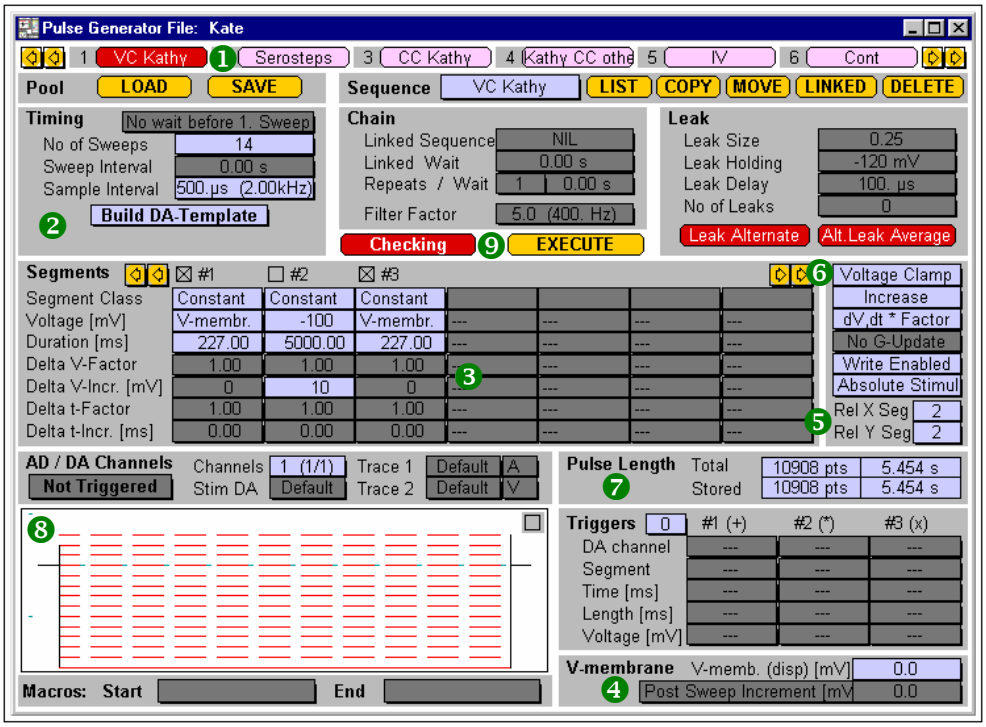

Fig. 5. The *Pulse Generator* Window showing the Pulse Protocol. This window was accessed by choosing Pulse Generator from the Pulse drop-down menu on *PULSE* main screen toolbar. In this window a Pulse Protocol is generated where the *PULSE* operator can predefine ❶ the desired cellular electrical stimulus so that it can later be used instantaneously during experimentation. The Timing section ❷ defined the number of stimulus Sweeps applied to the cell (14) and the frequency with which data is collected during each Sweep (once every 500 µs). Values in the Segments section ❸ defined the stimulus pattern internally for each Sweep, as well as the pattern between Sweeps. Here three Segments were defined, where Segments 1&3 were 227.0 ms Resting Phases with no electrical stimulation, while Segment 2 was the Stimulus Phase where for 5000 ms an electrical stimulus of -100 mV was initially applied to the cell. Subsequent Sweep Stimulation Phases increased by +10 mV so that the final Sweep stimulated at +30 mV. The holding membrane potential was defined as 0 mV ❹ because symmetrical Na^+ solutions were used during experimentation. The Relevant Segments ❺ for data retrieval were defined so that later data analysis used information collected from Segment 2 only, and the type of patch-clamping mode ❻ was selected here (i.e. either voltage-clamping or current-clamping). The total number of data points and the time for each Sweep was indicated in the Pulse Length Segment ❼ and the entire Protocol displayed diagrammatically ❽ for easy reference. Once the Protocol was defined was checked for errors by initiating the Checking sequence ❾ and the entire Protocol was complete and ready for use.

2.5 Data analysis

Each experiment in a given condition was carried out minimum of five times and the mean was determined as the representative result. Each condition was thus tested in at least 3 separate experiments. The average and the standard errors were calculated for the experimental values and analysed statistically by using Sigma Plot software (SDR Incorporation). Slopes of linear regressions were analysed by t-test.

3. Results

Electrophysiological heterogeneity of the B103 cell-line was observed where channel current responses divided the cells into three groups: with low, medium, and high conductance. There was no correlation between conductance and morphology because the cells used were morphologically identical as well as culture incubation time.

3.1 B103 currents in physiological solution

Cells were examined via the patch-clamp technique first in physiological solutions where K^+ was the primary cationic component of the pipette solution, imitating the internal and external conditions found *in vivo.* Throughout the course of the experimental series, all patch-clamp recordings were taken at a constant temperature of 22°C unless otherwise indicated. The average value of resting membrane potential for B103 cells in physiological saline was - 68 ± 3 mV close to potassium reversal potential expected for cells of neuronal origin.

Single-channel recordings in cell attached configurations in mammalian Ringer solution (Figure#6) gave a maximum conductance, of 0.44 nS, at 30 mV. The calculated ±30 mV slope conductance (the average conductance at +30 mV divided by the average conductance at -30 mV) was 1.02.

Subsequent Protocol applications showed a trend for decreasing current responses to the maximum applied potential from that initially recorded for each cell.

3.2 B103 Currents in symmetrical ionic concentration

The second set of solutions (with same sodium concentration on both sides) used during experiments gave a resting membrane potential of close to 0 mV. The presence of three subsets of conductances of B103 cells noted were based on their whole-cell current responses observed under symmetrical solutions.

3.2.1 The low conductance subset – Control in symmetrical solutions

These cells were categorised based on their current response to the maximum hyperpolarising step in the Protocol, that is at -100mV. Responses that were observed to be of 30 pA or less were categorised into this subset.

Whole-cell recordings were taken under symmetrical solutions (Figure#7) giving an average maximum conductance value of 0.28 nS at +30 mV. The calculated E_{rev} was -0.13 mV, while the calculated ±30 mV slope conductance was 1.08, indicating rather linear relationship between voltages and the current responses.

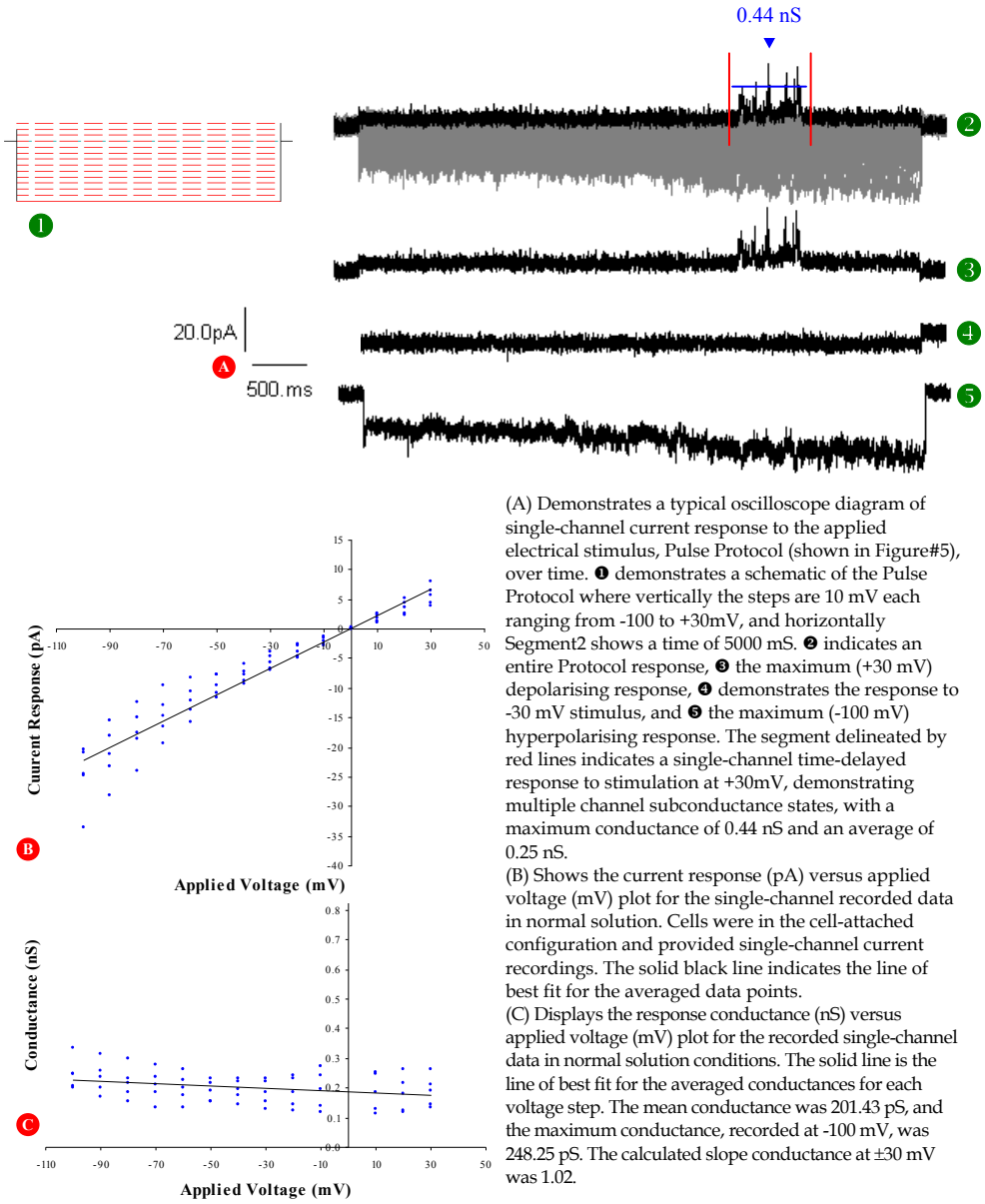

(A) Demonstrates a typical oscilloscope diagram of single-channel current response to the applied electrical stimulus, Pulse Protocol (shown in Figure#5), over time. ❶ demonstrates a schematic of the Pulse Protocol where vertically the steps are 10 mV each ranging from -100 to +30mV, and horizontally Segment2 shows a time of 5000 mS. ❷ indicates an entire Protocol response, ❸ the maximum (+30 mV) depolarising response, ❹ demonstrates the response to -30 mV stimulus, and ❺ the maximum (-100 mV) hyperpolarising response. The segment delineated by red lines indicates a single-channel time-delayed response to stimulation at +30mV, demonstrating multiple channel subconductance states, with a maximum conductance of 0.44 nS and an average of 0.25 nS.
(B) Shows the current response (pA) versus applied voltage (mV) plot for the single-channel recorded data in normal solution. Cells were in the cell-attached configuration and provided single-channel current recordings. The solid black line indicates the line of best fit for the averaged data points.
(C) Displays the response conductance (nS) versus applied voltage (mV) plot for the recorded single-channel data in normal solution conditions. The solid line is the line of best fit for the averaged conductances for each voltage step. The mean conductance was 201.43 pS, and the maximum conductance, recorded at -100 mV, was 248.25 pS. The calculated slope conductance at ±30 mV was 1.02.

Fig. 6. Single-Channel Control Results from B103 Cells Recorded in Normal Physiological Solutions: 137/3.7 $[Na^+]_o/[Na^+]_i$. All recordings were taken at a temperature of 20°C.

From this low conductance subset of B103 cells, two whole-cell current responses were observed: fast transient current (Figure#7*) and slow steady-state responses, where the amplitude and duration varied significantly. Fast transient currents were seen at the initiation of a voltage step and had a duration of 5-7 ms with a peak current, at maximum hyperpolarising potential, of -43.01 pA, while the slow steady-state current showed a greater duration of 4993-4995 ms. The average current recorded for the steady-state response was -20.64 pA. While subsequent current responses varied in amplitude, the durations were seen to remain constant unless otherwise indicated.

3.2.2 The medium conductance subset – Control in symmetrical solutions

The maximum average whole-cell conductance recorded from the B103 medium subset with experimental solutions (Figure#8) was 0.97 nS at + 30 mV. The calculated E_{rev} was -3.32 mV, while the calculated ±30 mV slope conductance was 1.4. Responses that were observed to be between 30-100 pA at -100 mV were categorised into the medium subset.

3.2.3 The high conductance subset – Control in symmetrical solutions

The average maximum control whole-cell conductance recorded for the high B103 subset with experimental solutions (Figure #9) was 1.39 nS at +30 mV. The calculated E_{rev} was 0.57 mV, while the calculated ±30 mV slope conductance was 1.09. Current response observed at -100 mV was greater than 100 pA in this high subset of B103 cells.

3.3 Serotonin receptor channel currents in B103 cell

Serotonin in different concentrations (10 μM , 500 μM & 1mM) was applied to low medium and high subsets of B103 cells. Serotonin gated currents were observed in B103 cells in the presence of 1 μM TTX.

3.3.1 Serotonin receptor channel currents in B103 cell (Low conductance subset)

The mean maximum whole-cell conductance recorded from low B103 cells in response to transient, externally applied serotonin (5-HT) in symmetrical sodium solutions (10 μM, Figure#10) was seen at +30 mV to be of 0.30 nS. The calculated E_{rev} was 0.34 mV, while the calculated ±30 mV slope conductance was 1.09. At maximum hyperpolarisation the fast transient peak was -86.30 pA and the steady-state response was -29.61 pA.

Where as in the presence of 500 μM (Figure#12) the maximum mean whole-cell conductance recorded from the low subset of B103 cells was 0.42 nS at +30 mV. The calculated Erev was 0.81 mV, while the calculated ±30 mV slope conductance was 1.24.

The maximal current value for the 440 ms fast transient was -40.28 pA and the average for then 4560 ms steady-state response was -25.0 pA.

3.3.2 Serotonin receptor channel currents in B103 cell (Medium conductance subset)

The maximal average whole-cell conductance recorded from the medium subset of B103 cells in response to external transiently applied 10 μM 5-HT with symmetrical solutions (Figure#11) was 3.09 nS at +30 mV. The calculated Erev was 13.91 mV, while the calculated ±30 mV slope conductance was 2.35.

Low B103 Subset Response to Transient Bath Application of 5-HT in Symmetrical Solutions

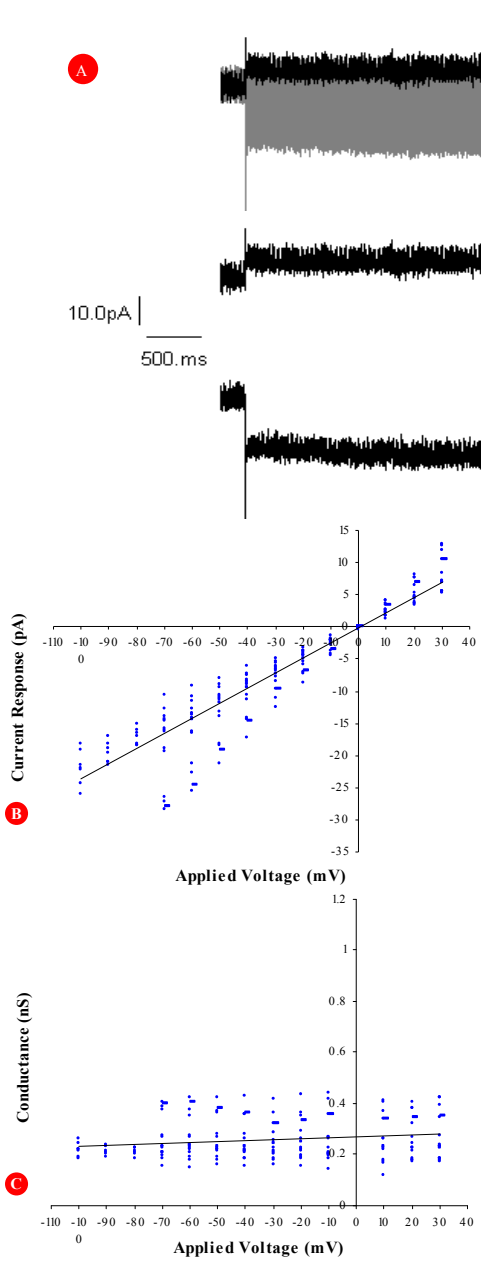

(A) Demonstrates a typical oscilloscope diagram of the whole-cell current response to the applied voltages. ❷ indicates an entire Protocol response, ❸ the maximum (+30 mV) depolarising response, and ❹ the maximum (-100 mV) hyperpolarising response. Importantly the spikes seen at the initiation and discontinuation of Segment2 are not capacitative transients as these values were rectified for during recording. From the recorded response data two types of B103 current response can be identified: fast transient current (*) and slow steady-state responses.
(B) Shows the current response (pA) versus applied voltage (mV) plot for the whole-cell recorded data in experimental solutions. The solid black line indicates the line of best fit for the averaged data points. The reversal potential calculated from the plotted data was -0.13 mV, with a mean current at +30 mV of -7.72 pA.
(C) Displays the response conductance (nS) versus applied voltage (mV) plot for the recorded whole-cell data in symmetrical solution conditions. The solid line is the line of best fit for the averaged conductances for each voltage step. The mean conductance at -30 mV was 0.26 nS, and the maximum conductance, recorded at +30 mV, was 0.28 nS. The calculated slope conductance at ±30 mV was 0.24.

Fig. 7. Whole-Cell Control Recordings from the Low Subset of B103 Cells in Symmetrical Solutions: 140/140 $[Na^+]_o/[Na^+]_i$.

Medium B103 Subset Response to Transient Bath Application of 5-HT in Symmetrical Solutions

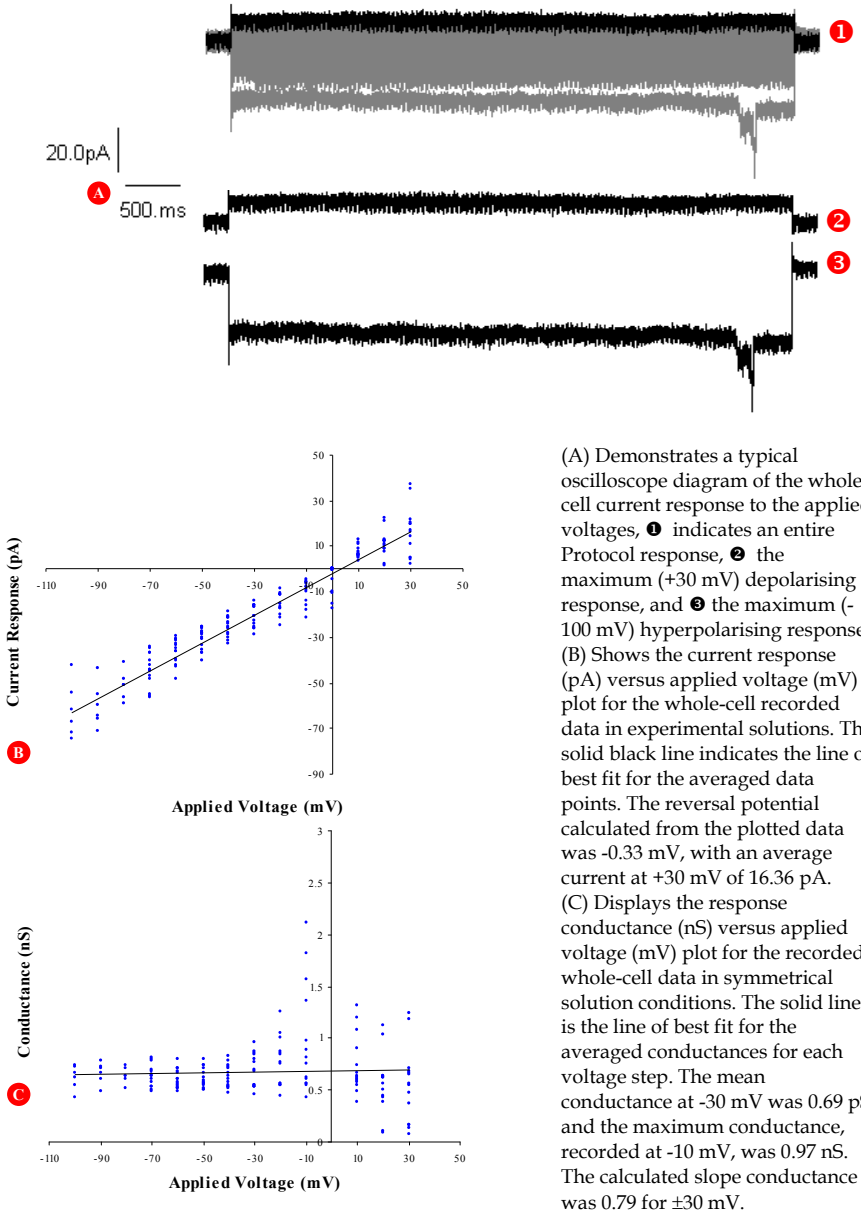

(A) Demonstrates a typical oscilloscope diagram of the whole-cell current response to the applied voltages, ❶ indicates an entire Protocol response, ❷ the maximum (+30 mV) depolarising response, and ❸ the maximum (-100 mV) hyperpolarising response. (B) Shows the current response (pA) versus applied voltage (mV) plot for the whole-cell recorded data in experimental solutions. The solid black line indicates the line of best fit for the averaged data points. The reversal potential calculated from the plotted data was -0.33 mV, with an average current at +30 mV of 16.36 pA. (C) Displays the response conductance (nS) versus applied voltage (mV) plot for the recorded whole-cell data in symmetrical solution conditions. The solid line is the line of best fit for the averaged conductances for each voltage step. The mean conductance at -30 mV was 0.69 pS, and the maximum conductance, recorded at -10 mV, was 0.97 nS. The calculated slope conductance was 0.79 for ±30 mV.

Fig. 8. Whole-Cell Control Recordings from the Medium Subset of B103 Cells in Symmetrical Solutions.

High B103 Subset Response to Transient Bath Application of 5-HT in Symmetrical Solutions

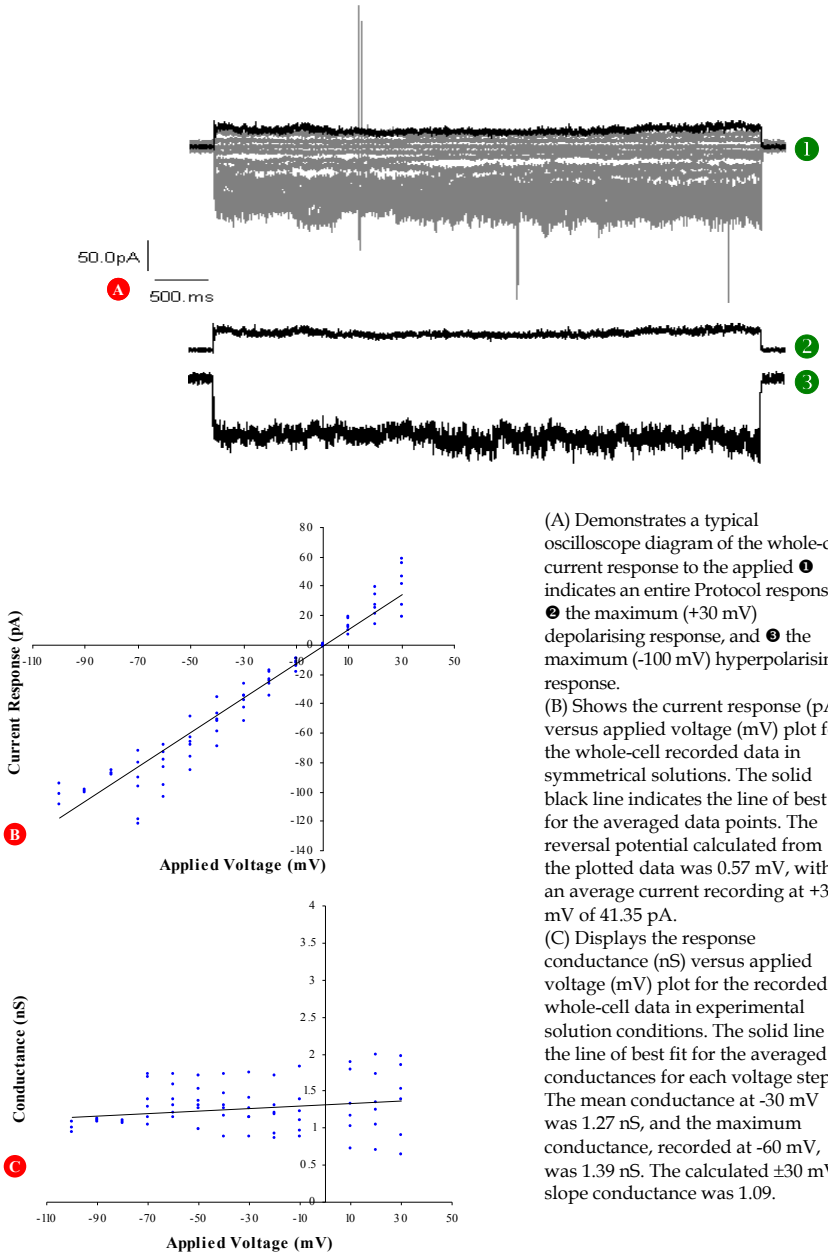

(A) Demonstrates a typical oscilloscope diagram of the whole-cell current response to the applied ❶ indicates an entire Protocol response, ❷ the maximum (+30 mV) depolarising response, and ❸ the maximum (-100 mV) hyperpolarising response.
(B) Shows the current response (pA) versus applied voltage (mV) plot for the whole-cell recorded data in symmetrical solutions. The solid black line indicates the line of best fit for the averaged data points. The reversal potential calculated from the plotted data was 0.57 mV, with an average current recording at +30 mV of 41.35 pA.
(C) Displays the response conductance (nS) versus applied voltage (mV) plot for the recorded whole-cell data in experimental solution conditions. The solid line is the line of best fit for the averaged conductances for each voltage step. The mean conductance at -30 mV was 1.27 nS, and the maximum conductance, recorded at -60 mV, was 1.39 nS. The calculated ±30 mV slope conductance was 1.09.

Fig. 9. Whole-Cell Control Recordings from the High Subset of B103 Cells in Symmetrical Solutions.

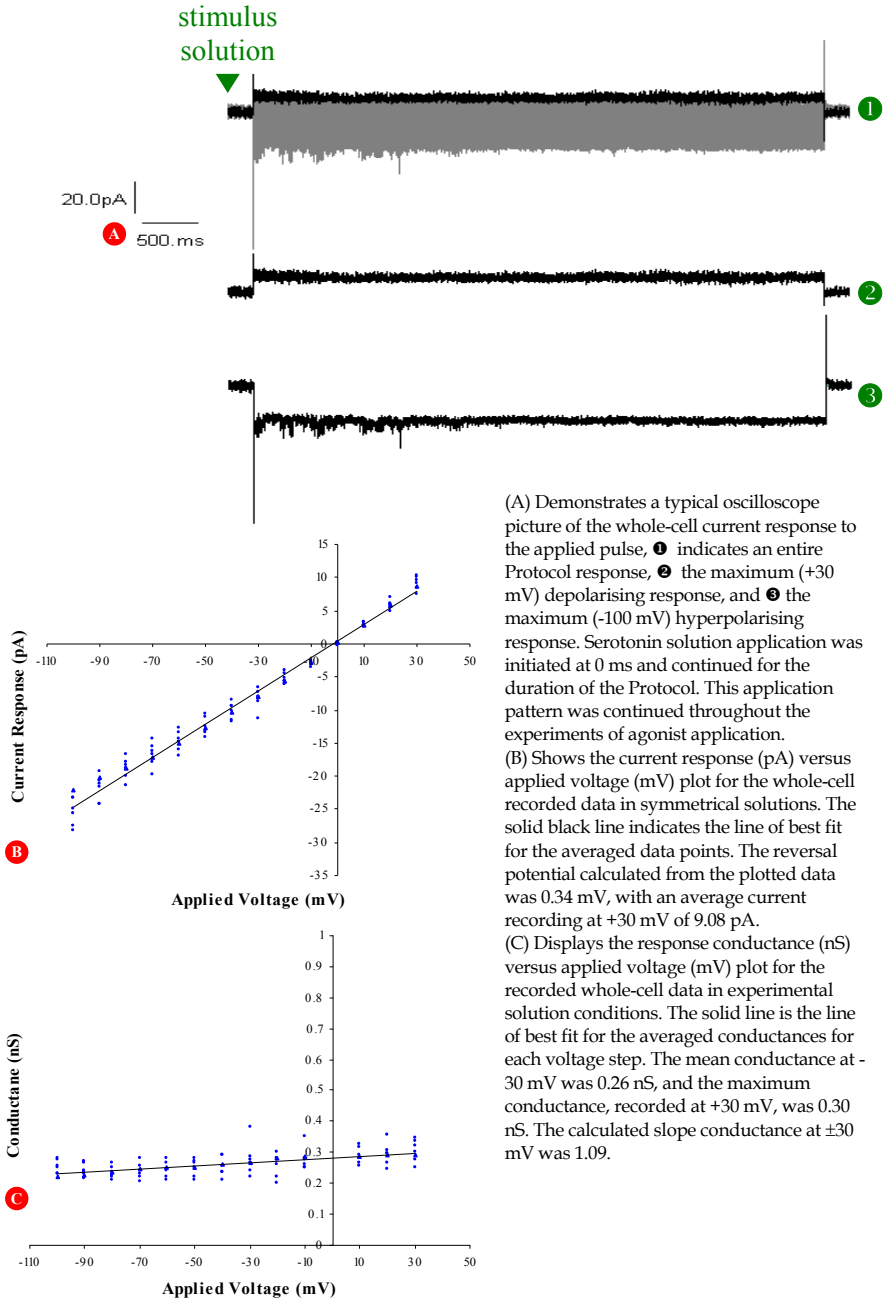

(A) Demonstrates a typical oscilloscope picture of the whole-cell current response to the applied pulse, ❶ indicates an entire Protocol response, ❷ the maximum (+30 mV) depolarising response, and ❸ the maximum (-100 mV) hyperpolarising response. Serotonin solution application was initiated at 0 ms and continued for the duration of the Protocol. This application pattern was continued throughout the experiments of agonist application.
(B) Shows the current response (pA) versus applied voltage (mV) plot for the whole-cell recorded data in symmetrical solutions. The solid black line indicates the line of best fit for the averaged data points. The reversal potential calculated from the plotted data was 0.34 mV, with an average current recording at +30 mV of 9.08 pA.
(C) Displays the response conductance (nS) versus applied voltage (mV) plot for the recorded whole-cell data in experimental solution conditions. The solid line is the line of best fit for the averaged conductances for each voltage step. The mean conductance at -30 mV was 0.26 nS, and the maximum conductance, recorded at +30 mV, was 0.30 nS. The calculated slope conductance at ±30 mV was 1.09.

Fig. 10. Whole-Cell Current Response of the Low B103 Subset to Transient Bath Application of 10 μM 5-HT in Symmetrical Solutions.

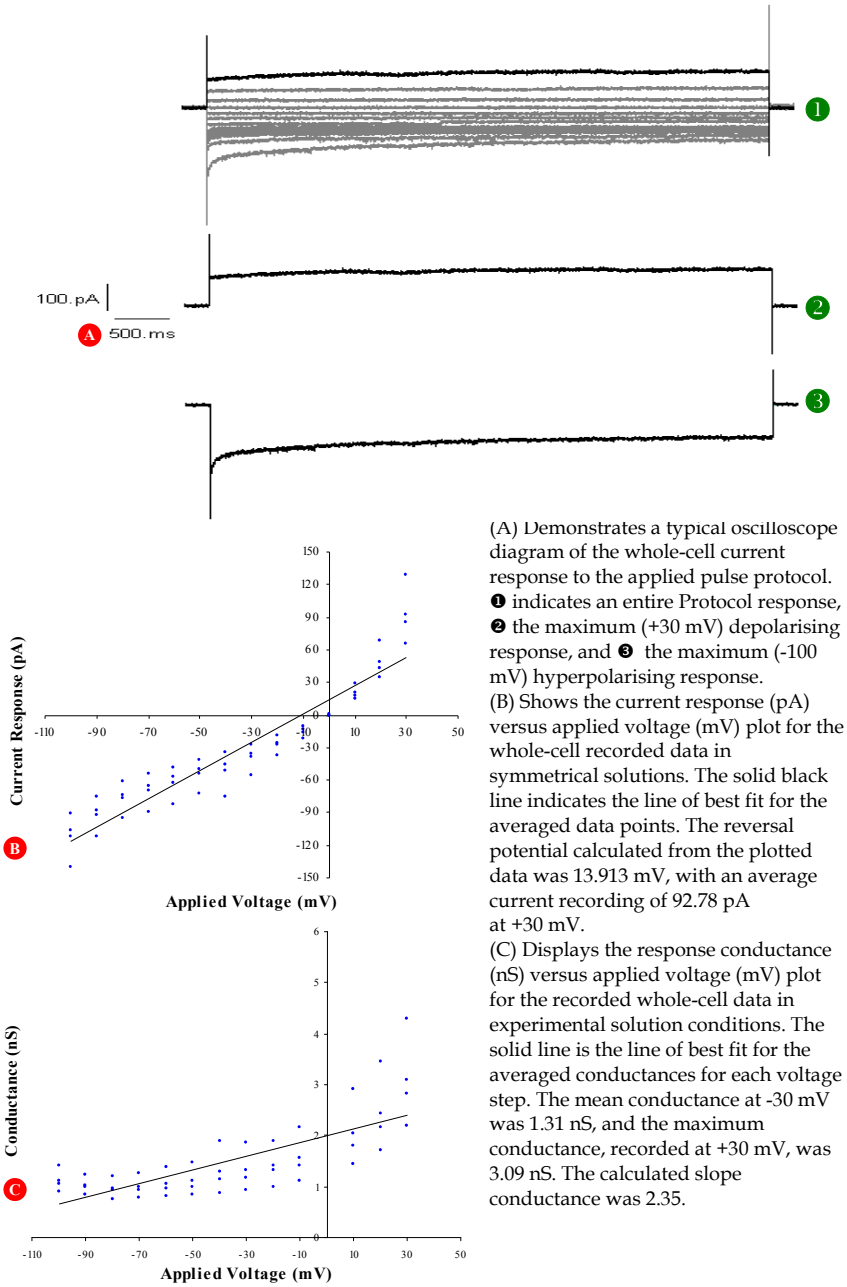

(A) Demonstrates a typical oscilloscope diagram of the whole-cell current response to the applied pulse protocol. ❶ indicates an entire Protocol response, ❷ the maximum (+30 mV) depolarising response, and ❸ the maximum (-100 mV) hyperpolarising response.
(B) Shows the current response (pA) versus applied voltage (mV) plot for the whole-cell recorded data in symmetrical solutions. The solid black line indicates the line of best fit for the averaged data points. The reversal potential calculated from the plotted data was 13.913 mV, with an average current recording of 92.78 pA at +30 mV.
(C) Displays the response conductance (nS) versus applied voltage (mV) plot for the recorded whole-cell data in experimental solution conditions. The solid line is the line of best fit for the averaged conductances for each voltage step. The mean conductance at -30 mV was 1.31 nS, and the maximum conductance, recorded at +30 mV, was 3.09 nS. The calculated slope conductance was 2.35.

Fig. 11. Whole-Cell Current Response of the Medium B103 Subset to Transient Bath Application of 10 μM 5-HT in Symmetrical Solutions.

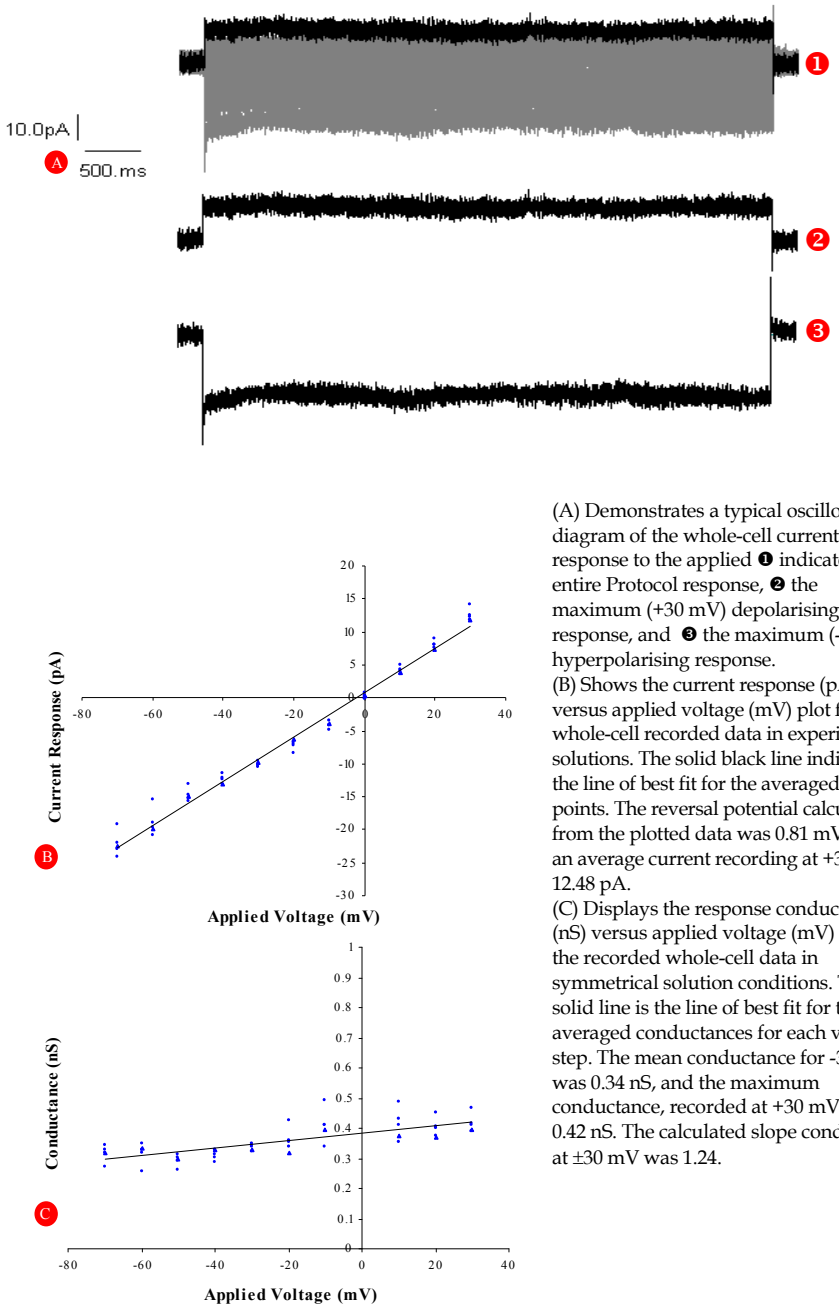

(A) Demonstrates a typical oscilloscope diagram of the whole-cell current response to the applied ❶ indicates an entire Protocol response, ❷ the maximum (+30 mV) depolarising response, and ❸ the maximum (-70 mV) hyperpolarising response.
(B) Shows the current response (pA) versus applied voltage (mV) plot for the whole-cell recorded data in experimental solutions. The solid black line indicates the line of best fit for the averaged data points. The reversal potential calculated from the plotted data was 0.81 mV, with an average current recording at +30 mV of 12.48 pA.
(C) Displays the response conductance (nS) versus applied voltage (mV) plot for the recorded whole-cell data in symmetrical solution conditions. The solid line is the line of best fit for the averaged conductances for each voltage step. The mean conductance for -30 mV was 0.34 nS, and the maximum conductance, recorded at +30 mV, was 0.42 nS. The calculated slope conductance at ±30 mV was 1.24.

Fig. 12. Whole-Cell Current Response of the Low B103 Subset to Transient Bath Application of 500 μM 5-HT in Symmetrical Solutions.

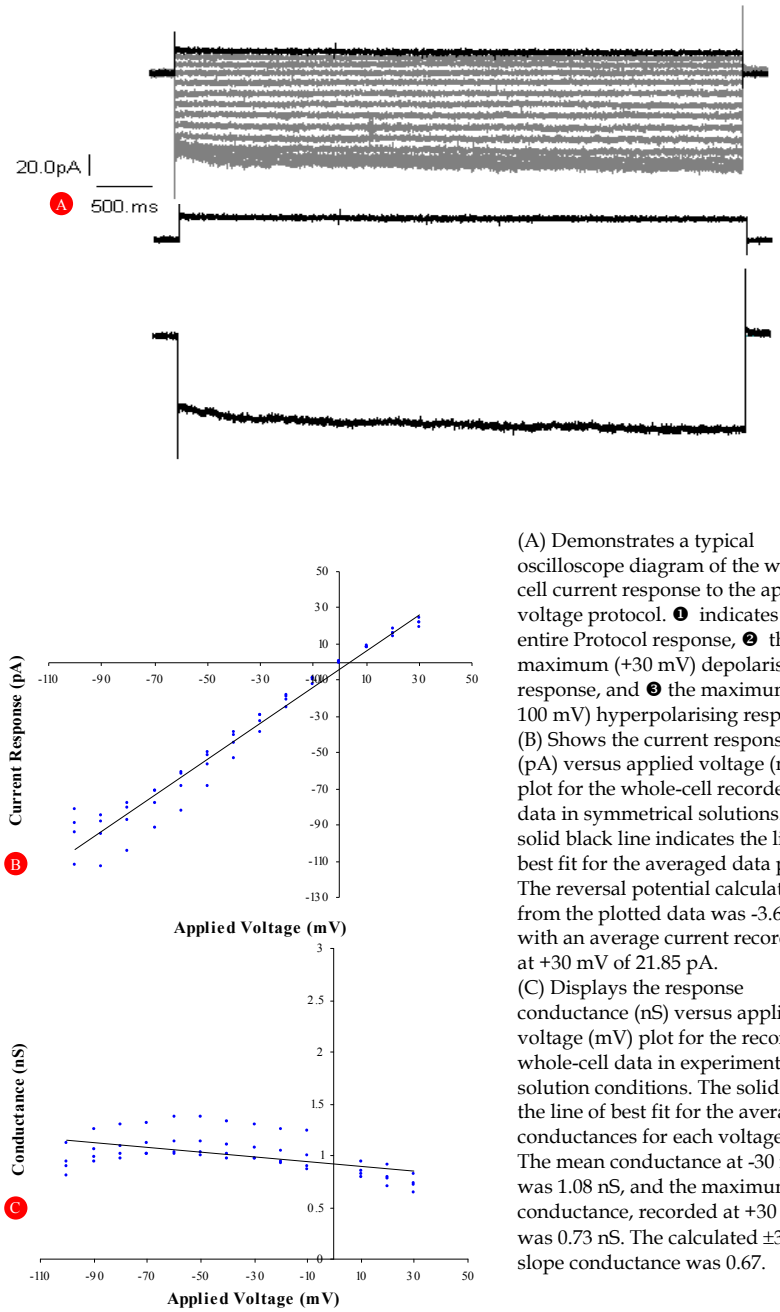

(A) Demonstrates a typical oscilloscope diagram of the whole-cell current response to the applied voltage protocol. ❶ indicates an entire Protocol response, ❷ the maximum (+30 mV) depolarising response, and ❸ the maximum (-100 mV) hyperpolarising response. (B) Shows the current response (pA) versus applied voltage (mV) plot for the whole-cell recorded data in symmetrical solutions. The solid black line indicates the line of best fit for the averaged data points. The reversal potential calculated from the plotted data was -3.64 mV, with an average current recording at +30 mV of 21.85 pA. (C) Displays the response conductance (nS) versus applied voltage (mV) plot for the recorded whole-cell data in experimental solution conditions. The solid line is the line of best fit for the averaged conductances for each voltage step. The mean conductance at -30 mV was 1.08 nS, and the maximum conductance, recorded at +30 mV, was 0.73 nS. The calculated ±30 mV slope conductance was 0.67.

Fig. 13. Whole-Cell Current Response of the Medium B103 Subset to Transient Bath Application of 500 μM 5-HT in Symmetrical Solutions.

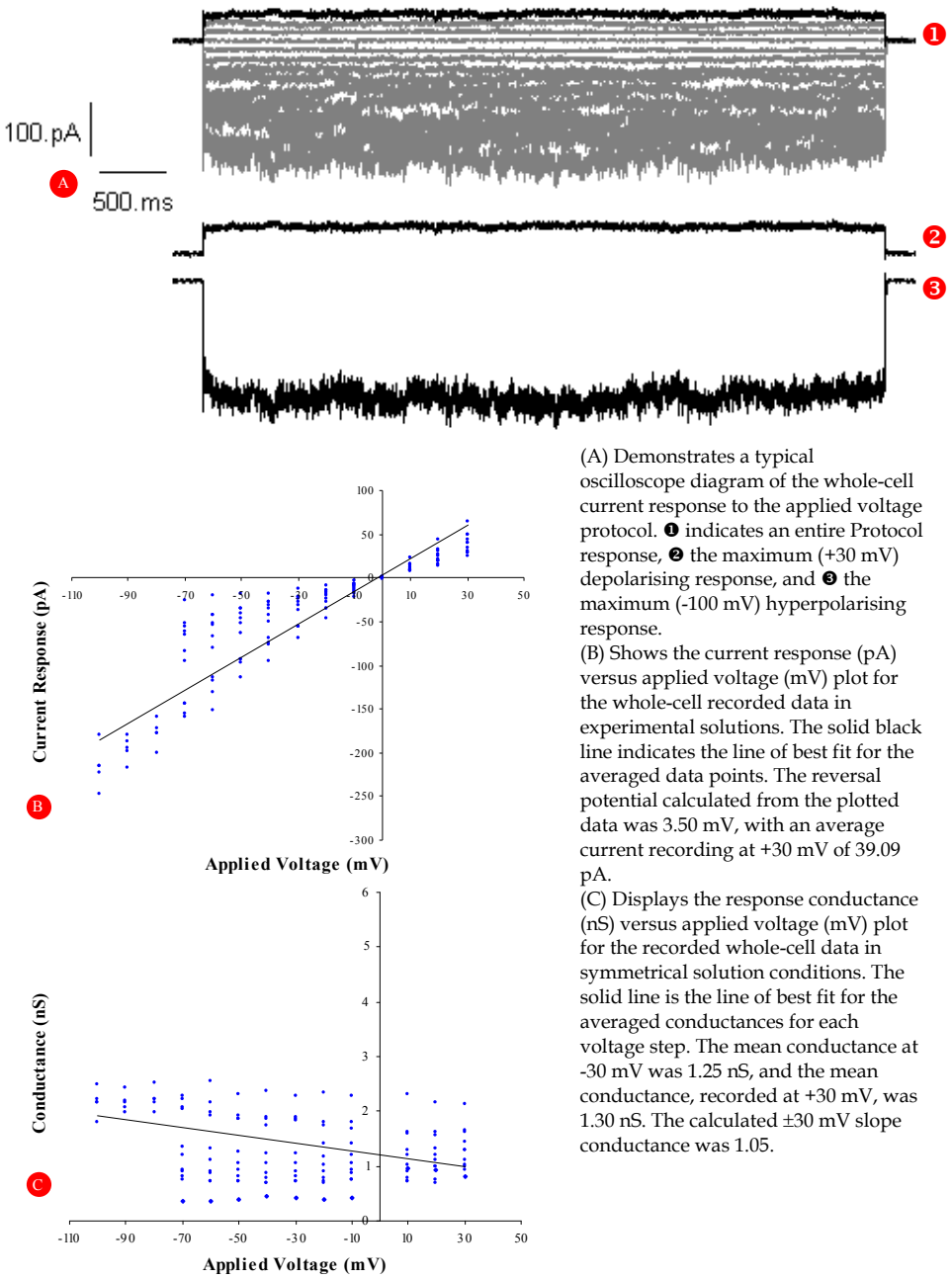

(A) Demonstrates a typical oscilloscope diagram of the whole-cell current response to the applied voltage protocol. ❶ indicates an entire Protocol response, ❷ the maximum (+30 mV) depolarising response, and ❸ the maximum (-100 mV) hyperpolarising response.
(B) Shows the current response (pA) versus applied voltage (mV) plot for the whole-cell recorded data in experimental solutions. The solid black line indicates the line of best fit for the averaged data points. The reversal potential calculated from the plotted data was 3.50 mV, with an average current recording at +30 mV of 39.09 pA.
(C) Displays the response conductance (nS) versus applied voltage (mV) plot for the recorded whole-cell data in symmetrical solution conditions. The solid line is the line of best fit for the averaged conductances for each voltage step. The mean conductance at -30 mV was 1.25 nS, and the mean conductance, recorded at +30 mV, was 1.30 nS. The calculated ±30 mV slope conductance was 1.05.

Fig. 14. Whole-Cell Current Response of the High B103 Subset to Transient Bath Application of 500 µM 5-HT in Symmetrical Solutions.

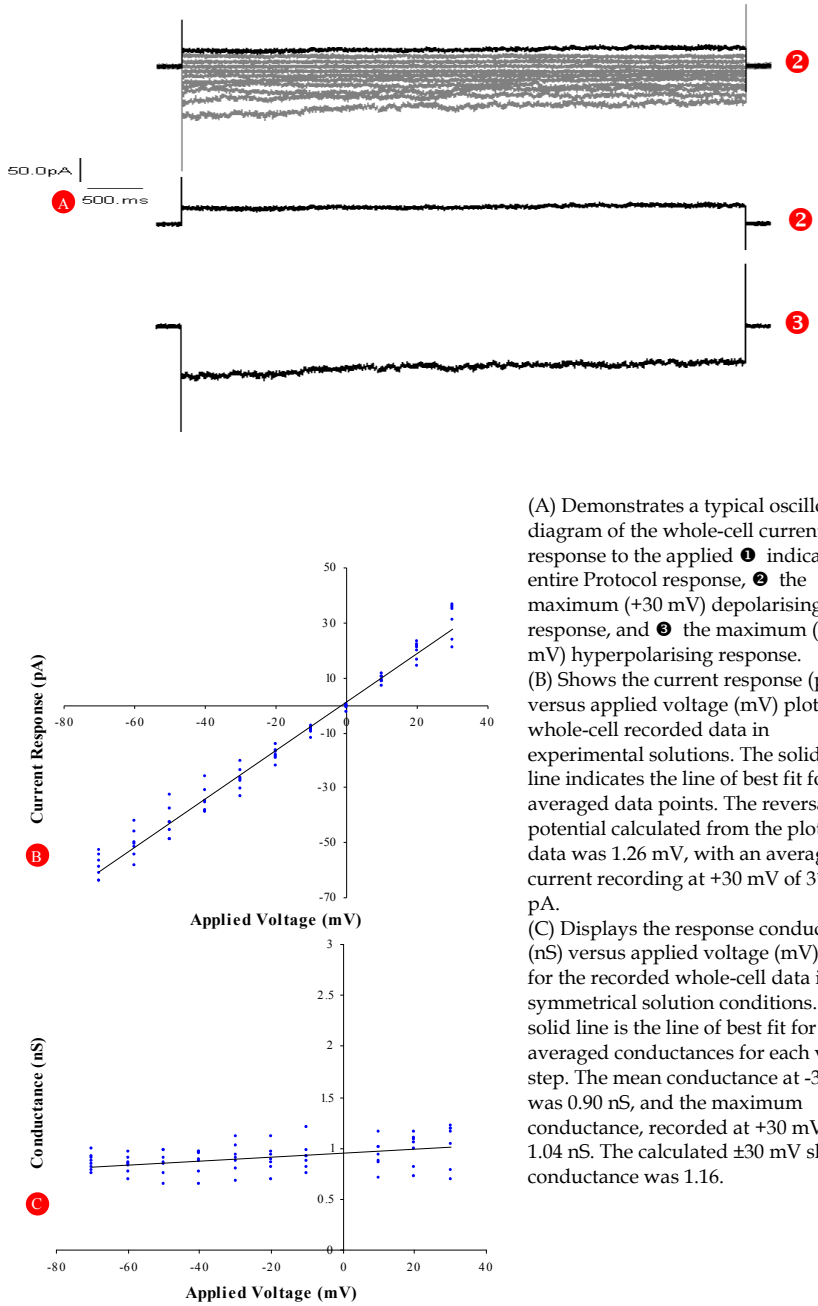

(A) Demonstrates a typical oscilloscope diagram of the whole-cell current response to the applied ❶ indicates an entire Protocol response, ❷ the maximum (+30 mV) depolarising response, and ❸ the maximum (-70 mV) hyperpolarising response.
(B) Shows the current response (pA) versus applied voltage (mV) plot for the whole-cell recorded data in experimental solutions. The solid black line indicates the line of best fit for the averaged data points. The reversal potential calculated from the plotted data was 1.26 mV, with an average current recording at +30 mV of 31.26 pA.
(C) Displays the response conductance (nS) versus applied voltage (mV) plot for the recorded whole-cell data in symmetrical solution conditions. The solid line is the line of best fit for the averaged conductances for each voltage step. The mean conductance at -30 mV was 0.90 nS, and the maximum conductance, recorded at +30 mV, was 1.04 nS. The calculated ±30 mV slope conductance was 1.16.

Fig. 15. Whole-Cell Current Response of the Low B103 Subset to Transient Bath Application of 1 mM 5-HT in Symmetrical Solutions.

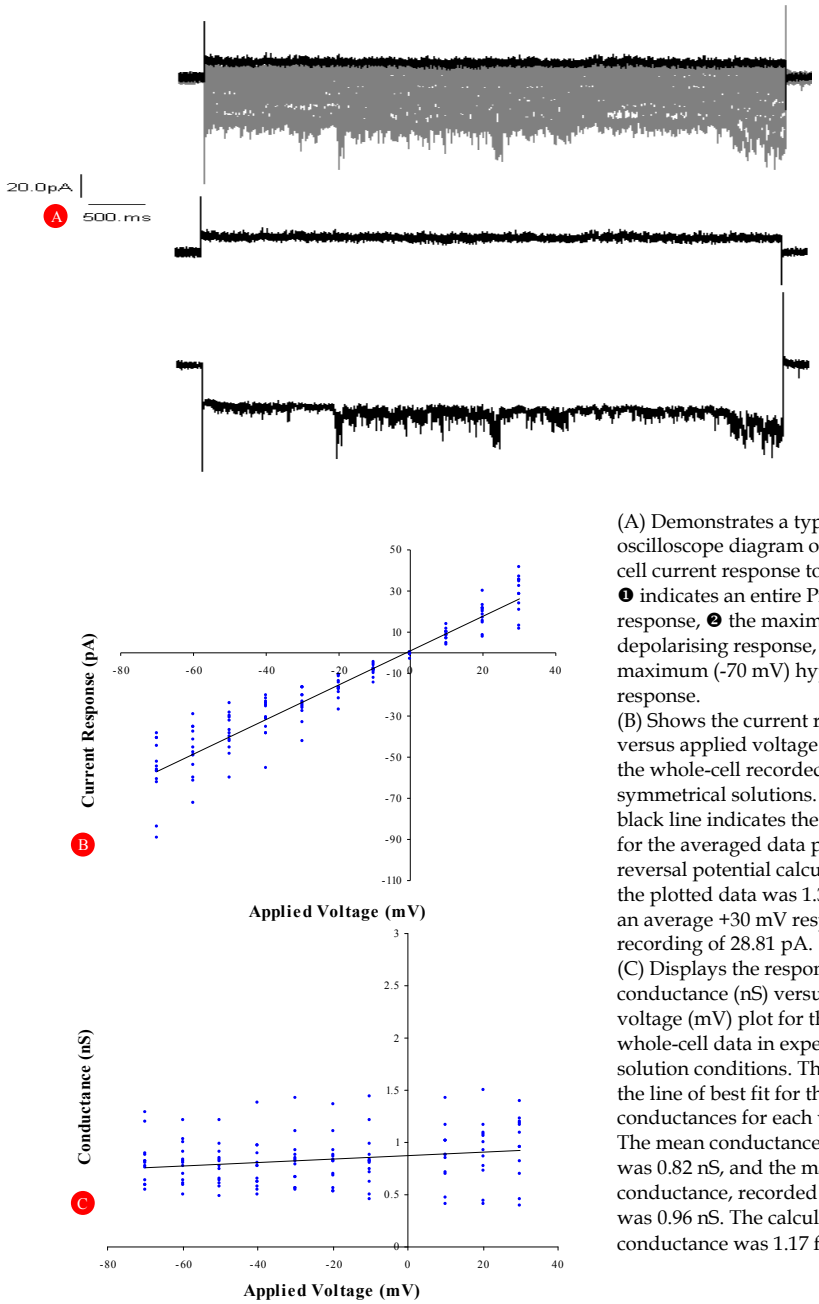

(A) Demonstrates a typical oscilloscope diagram of the whole-cell current response to the applied ❶ indicates an entire Protocol response, ❷ the maximum (+30 mV) depolarising response, and ❸ the maximum (-70 mV) hyperpolarising response.
(B) Shows the current response (pA) versus applied voltage (mV) plot for the whole-cell recorded data in symmetrical solutions. The solid black line indicates the line of best fit for the averaged data points. The reversal potential calculated from the plotted data was 1.33 mV, with an average +30 mV response current recording of 28.81 pA.
(C) Displays the response conductance (nS) versus applied voltage (mV) plot for the recorded whole-cell data in experimental solution conditions. The solid line is the line of best fit for the averaged conductances for each voltage step. The mean conductance at -30 mV was 0.82 nS, and the maximum conductance, recorded at +30 mV, was 0.96 nS. The calculated slope conductance was 1.17 for ±30 mV.

Fig. 16. Whole-Cell Current Response of the Medium B103 Subset to Transient Bath Application of 1 mM 5-HT in Symmetrical Solutions.

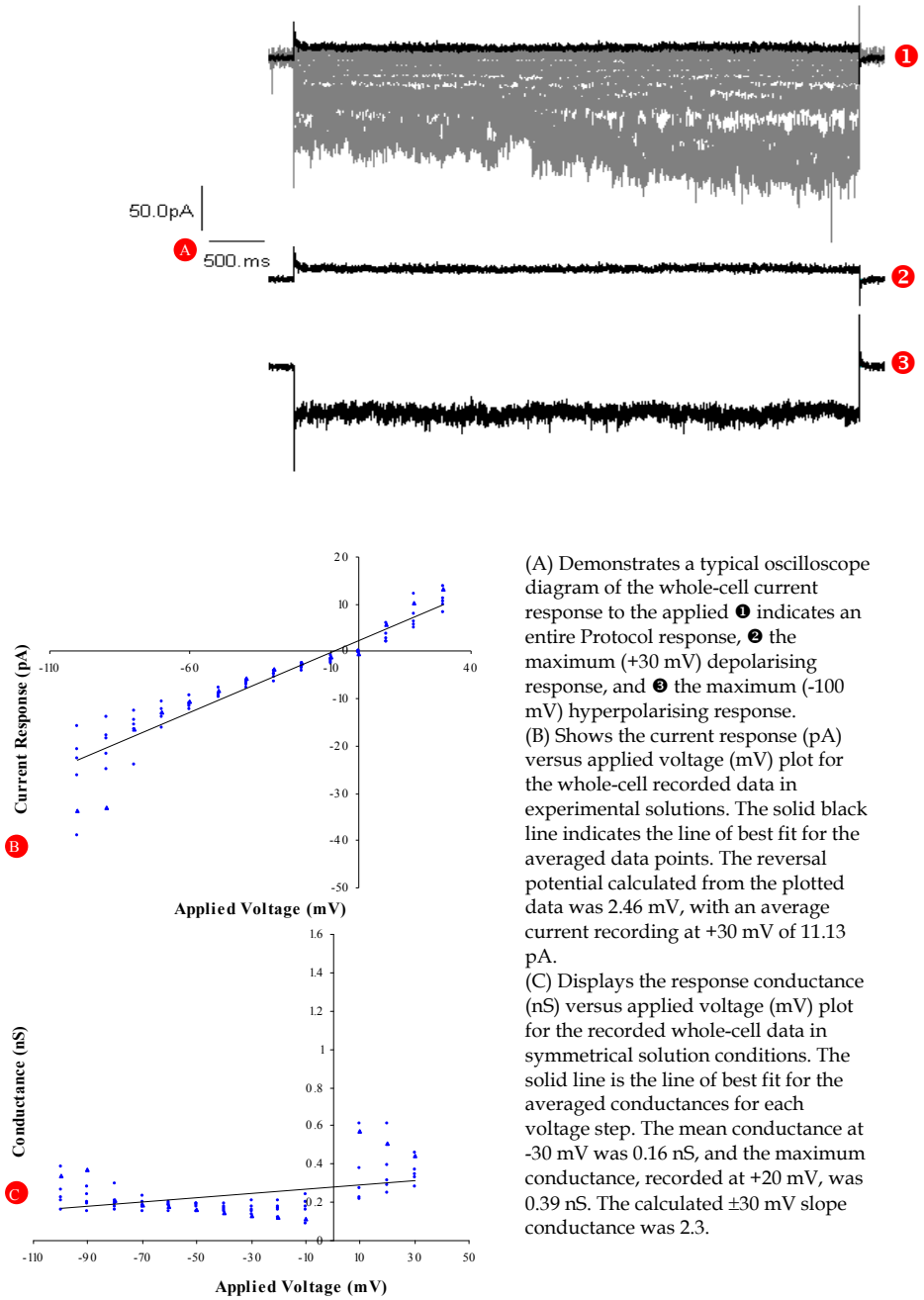

(A) Demonstrates a typical oscilloscope diagram of the whole-cell current response to the applied ❶ indicates an entire Protocol response, ❷ the maximum (+30 mV) depolarising response, and ❸ the maximum (-100 mV) hyperpolarising response.
(B) Shows the current response (pA) versus applied voltage (mV) plot for the whole-cell recorded data in experimental solutions. The solid black line indicates the line of best fit for the averaged data points. The reversal potential calculated from the plotted data was 2.46 mV, with an average current recording at +30 mV of 11.13 pA.
(C) Displays the response conductance (nS) versus applied voltage (mV) plot for the recorded whole-cell data in symmetrical solution conditions. The solid line is the line of best fit for the averaged conductances for each voltage step. The mean conductance at -30 mV was 0.16 nS, and the maximum conductance, recorded at +20 mV, was 0.39 nS. The calculated ±30 mV slope conductance was 2.3.

Fig. 17. Whole-Cell Current Response of the Low B103 Subset to Transient Bath Application of 5 μM D-Tubocurarine in Symmetrical Solutions.

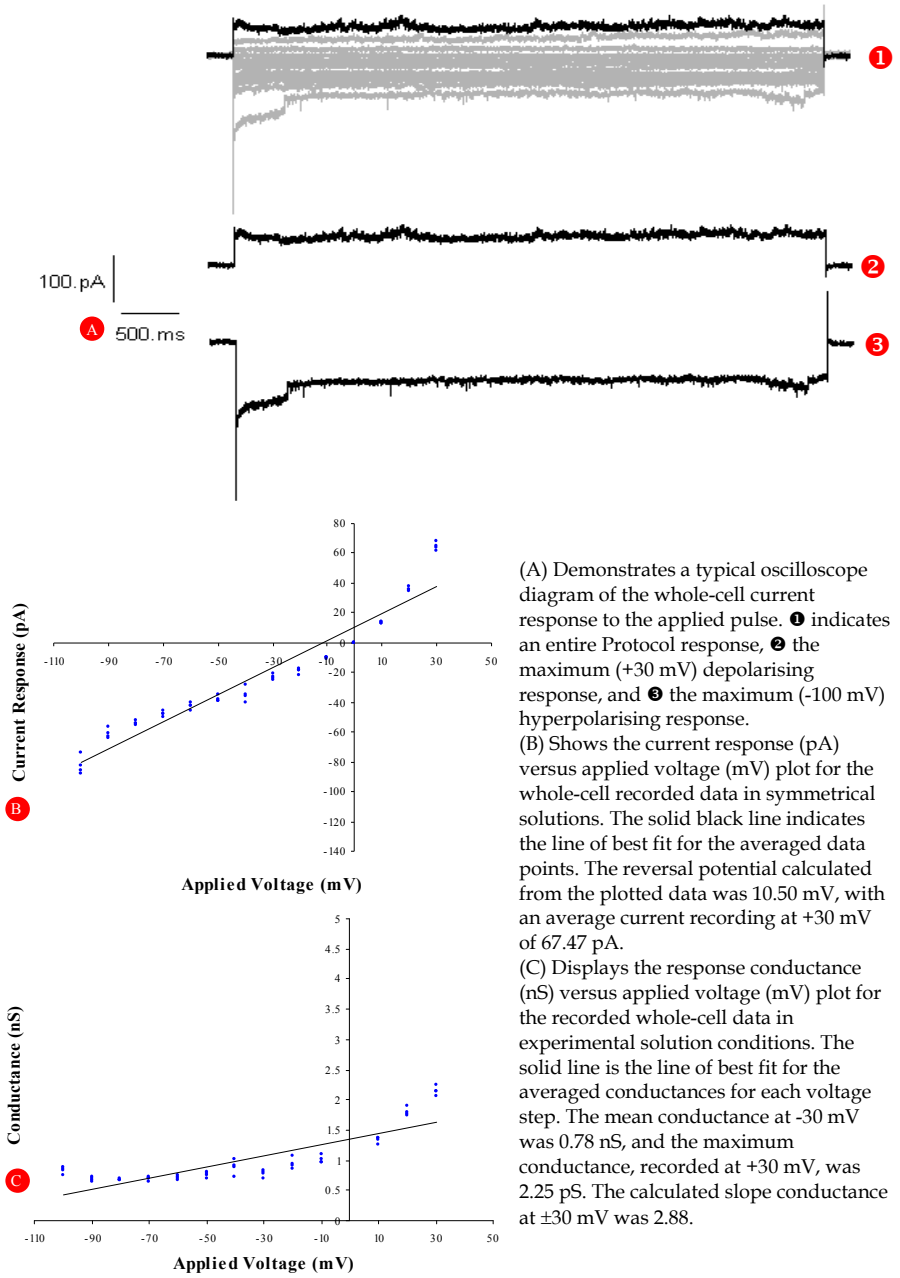

(A) Demonstrates a typical oscilloscope diagram of the whole-cell current response to the applied pulse. ❶ indicates an entire Protocol response, ❷ the maximum (+30 mV) depolarising response, and ❸ the maximum (-100 mV) hyperpolarising response.
(B) Shows the current response (pA) versus applied voltage (mV) plot for the whole-cell recorded data in symmetrical solutions. The solid black line indicates the line of best fit for the averaged data points. The reversal potential calculated from the plotted data was 10.50 mV, with an average current recording at +30 mV of 67.47 pA.
(C) Displays the response conductance (nS) versus applied voltage (mV) plot for the recorded whole-cell data in experimental solution conditions. The solid line is the line of best fit for the averaged conductances for each voltage step. The mean conductance at -30 mV was 0.78 nS, and the maximum conductance, recorded at +30 mV, was 2.25 pS. The calculated slope conductance at ±30 mV was 2.88.

Fig. 18. Whole-Cell Current Response of the Medium B103 Subset to Transient Bath Application of 5 μM D-Tubocurarine in Symmetrical Solutions.

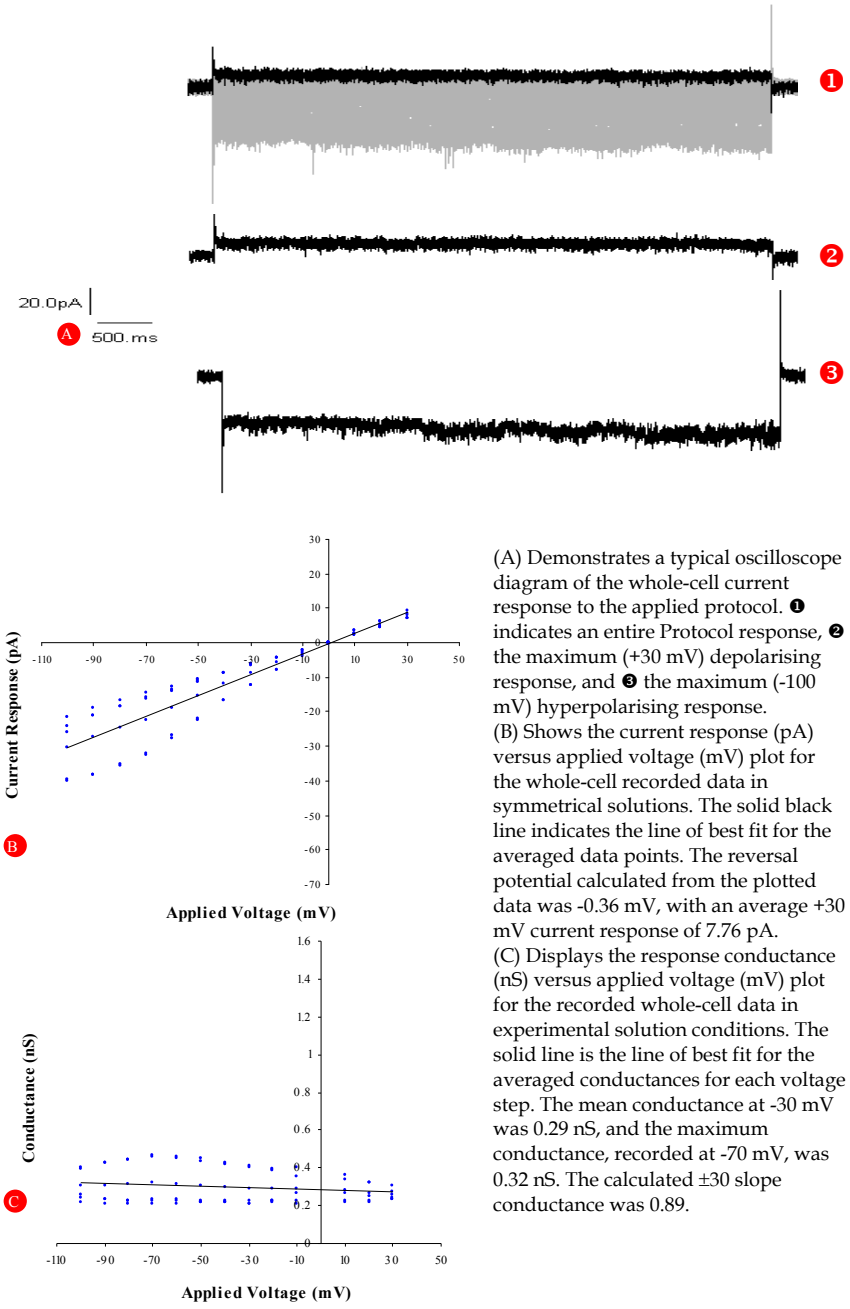

(A) Demonstrates a typical oscilloscope diagram of the whole-cell current response to the applied protocol. ❶ indicates an entire Protocol response, ❷ the maximum (+30 mV) depolarising response, and ❸ the maximum (-100 mV) hyperpolarising response.
(B) Shows the current response (pA) versus applied voltage (mV) plot for the whole-cell recorded data in symmetrical solutions. The solid black line indicates the line of best fit for the averaged data points. The reversal potential calculated from the plotted data was -0.36 mV, with an average +30 mV current response of 7.76 pA.
(C) Displays the response conductance (nS) versus applied voltage (mV) plot for the recorded whole-cell data in experimental solution conditions. The solid line is the line of best fit for the averaged conductances for each voltage step. The mean conductance at -30 mV was 0.29 nS, and the maximum conductance, recorded at -70 mV, was 0.32 nS. The calculated ±30 slope conductance was 0.89.

Fig. 19. Whole-Cell Current Response of the Low B103 Subset to Transient Bath Application of 5 µM D-Tubocurarine and 10 µM 5-HT in Symmetrical Solutions.

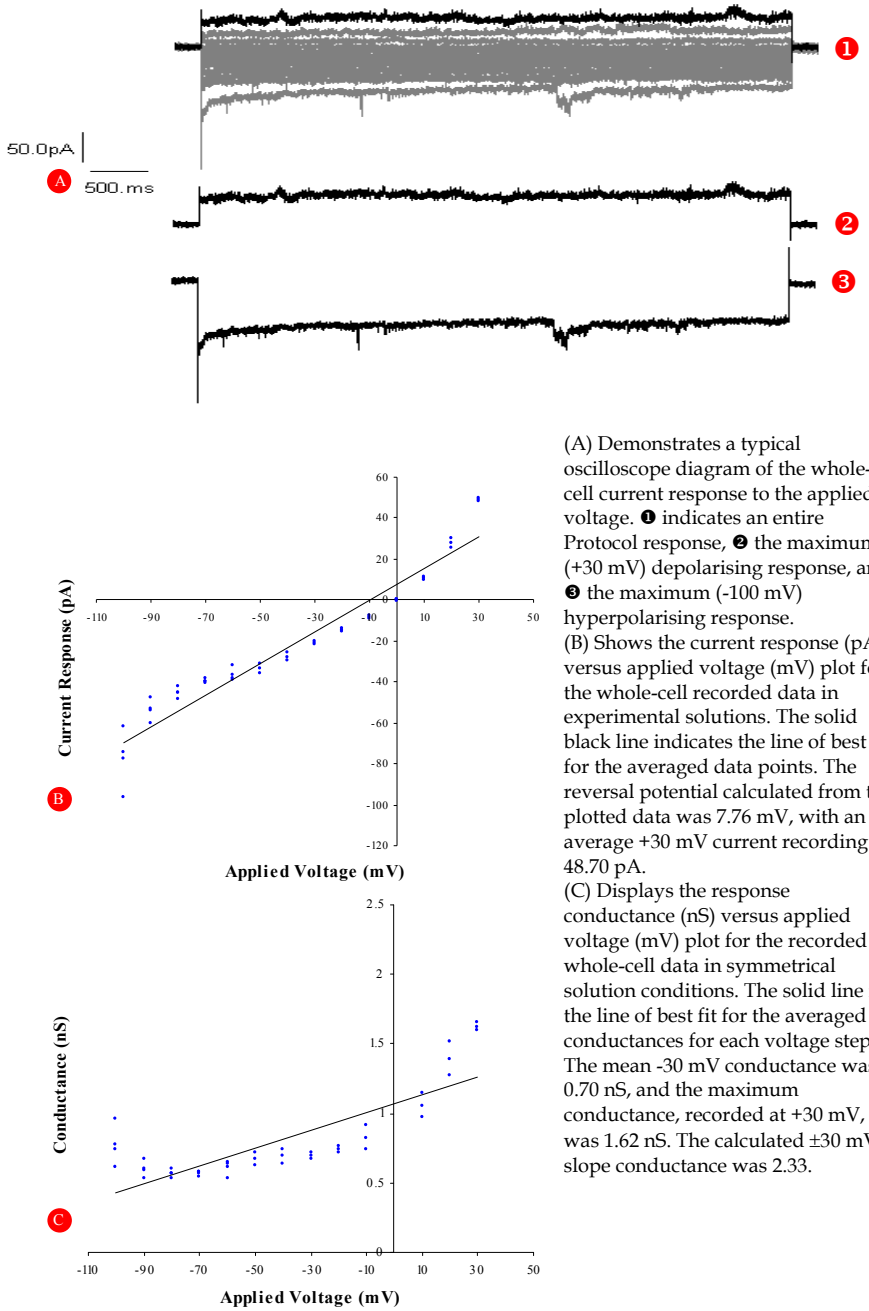

(A) Demonstrates a typical oscilloscope diagram of the whole-cell current response to the applied voltage. ❶ indicates an entire Protocol response, ❷ the maximum (+30 mV) depolarising response, and ❸ the maximum (-100 mV) hyperpolarising response.
(B) Shows the current response (pA) versus applied voltage (mV) plot for the whole-cell recorded data in experimental solutions. The solid black line indicates the line of best fit for the averaged data points. The reversal potential calculated from the plotted data was 7.76 mV, with an average +30 mV current recording of 48.70 pA.
(C) Displays the response conductance (nS) versus applied voltage (mV) plot for the recorded whole-cell data in symmetrical solution conditions. The solid line is the line of best fit for the averaged conductances for each voltage step. The mean -30 mV conductance was 0.70 nS, and the maximum conductance, recorded at +30 mV, was 1.62 nS. The calculated ±30 mV slope conductance was 2.33.

Fig. 20. Whole-Cell Current Response of the Medium B103 Subset to Transient Bath Application of 5 μM D-Tubocurarine and 10 μM 5-HT in Symmetrical Solutions.

		Mean Current (pA)		Mean g (nS)		Max g (nS)		Most	Slope g
		@ -30 mV	@ +30 mV	@ -30 mV	@ +30 mV	@ mV		Frequent g	@ ±30m
Normal Solutions		-5.57	5.67	0.19	0.19	0.25	-100	0.18	1.02
Symmetrical Solutions									
controls	Low	-7.72	8.31	0.26	0.28	0.28	+30	0.27	1.08
	Medium	-20.61	16.36	0.69	0.55	0.97	-10	0.63	0.80
	High	-37.98	41.35	1.27	1.38	1.39	-60	1.30	1.09
10 uM 5-HT	Low	-8.34	9.08	0.28	0.30	0.30	+30	0.24	1.09
	Medium	-39.41	92.78	1.31	3.09	3.09	+30	1.30	2.35
500 uM 5-HT	Low	-10.10	12.48	0.34	0.42	0.42	+30	0.32	1.24
	Medium	-32.43	21.85	1.08	0.73	1.14	-60	1.10	0.67
	High	-37.35	39.09	1.25	1.30	2.22	-80	1.20	1.05
1 mM 5-HT	Low	-26.99	31.26	0.90	1.04	1.04	+30	0.94	1.16
	Medium	-24.52	28.81	0.82	0.96	0.96	+30	0.81	1.17
5 uM d-tubocurarine	Low	-4.87	11.13	0.16	0.37	0.39	+20	0.80	2.28
	Medium	-23.39	67.47	0.78	2.25	2.25	+30	0.70	2.88
5 uM d-tubocurarine	Low	-8.75	7.76	0.29	0.26	0.32	-70	0.32	0.89
+ 10 uM 5-HT	Medium	-20.86	48.70	0.70	1.62	1.62	+30	0.56	2.33

E_{rev} for solution components was derived using the Nernst Equation

Normal Solutions E_K = -78.34 mV; E_{Na} = 91.24 mV; E_{Ca} = 0.007 mV; E_{Cl} = -0.05 mV

Symmetrical Solutions E_K = n/a; E_{Na} = 0.0 mV; E_{Ca} = n/a; E_{Cl} = -107.69 mV

g = conductance

SVA = successive voltage applications

where D = decrease in current response from initial, I = increase, & B = both increase and decr

CRT = Current Response Type

SS = steady-state

Note that data in this table is tabulated from averaged information and therefore some discrepencies might be noted when spe

Table 2. B103 Electrophydiological Response Summary

Fast transients demonstrated a -423.20 pA response to -100 mV stimulation with a slower decay time than previously noted of 1000 ms. The steady state response then lasted for the remaining 4000 ms with an average current of -133.33 pA.

The maximal average whole-cell conductance recorded from the medium subset of B103 cells in response to transient externally applied 500 μM 5-HT with experimental solutions (Figure#13) was 1.39 nS at -60 mV. The calculated Erev was -3.64 mV and the calculated ±30 mV slope conductance was 0.67.

The 5-7 ms fast transient response to maximum hyperpolarisation was -133.21 pA with the steady-state component displaying an average -86.67 pA current response. However the steady-state transient displayed an initiation at approximately half-maximal then increased in response to reach the average current.

Consecutive Pulse Protocol applications showed a trend for maximum hyperpolarisation current response to decrease stepwise from that initially recorded for each cell.

3.3.3 Serotonin receptor channel currents in B103 cell (High conductance subset)

Exhibits Whole-Cell Current Response of the High B103 Subset to Transient Bath Application of 500 μM 5-HT (Figure#14) in Symmetrical Solutions, as 10 μM 5-HT was not able to produce any response in this sub set of B103 cells.

All serotonin concentrations except 500 μM and other drugs were applied to only low and medium subsets of B103 cells.

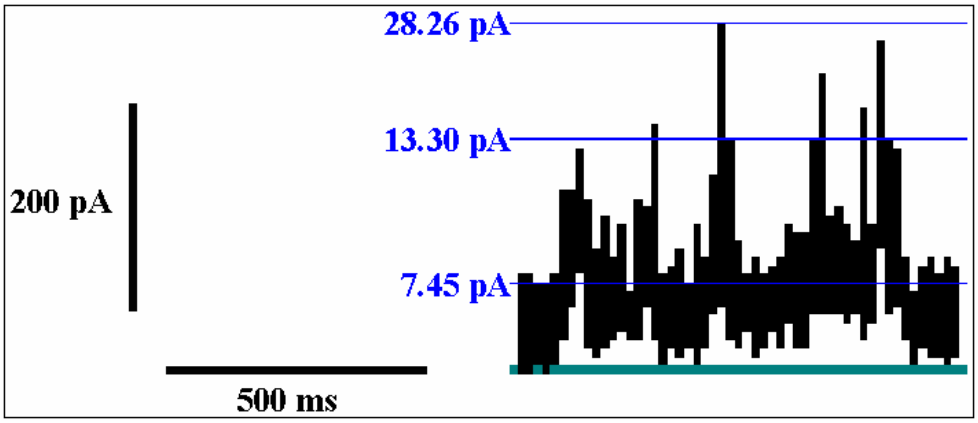

Fig. 21. Channel Subconductance States. This figure is a magnification of the area designated by vertical red lines in Figure#6 and represents a 837.50 ms alteration in the channel conducting state. As indicated in the figure by the horizontal blue lines, the max current recorded was 28.26 pA (0.88 nS), the average current was 7.45 (0.25nS), and the probable true maximum conductance state for the channel was when 13.30 pA of current was recorded (0.44 nS) – chosen on the basis of the number of peaks passing through the line.

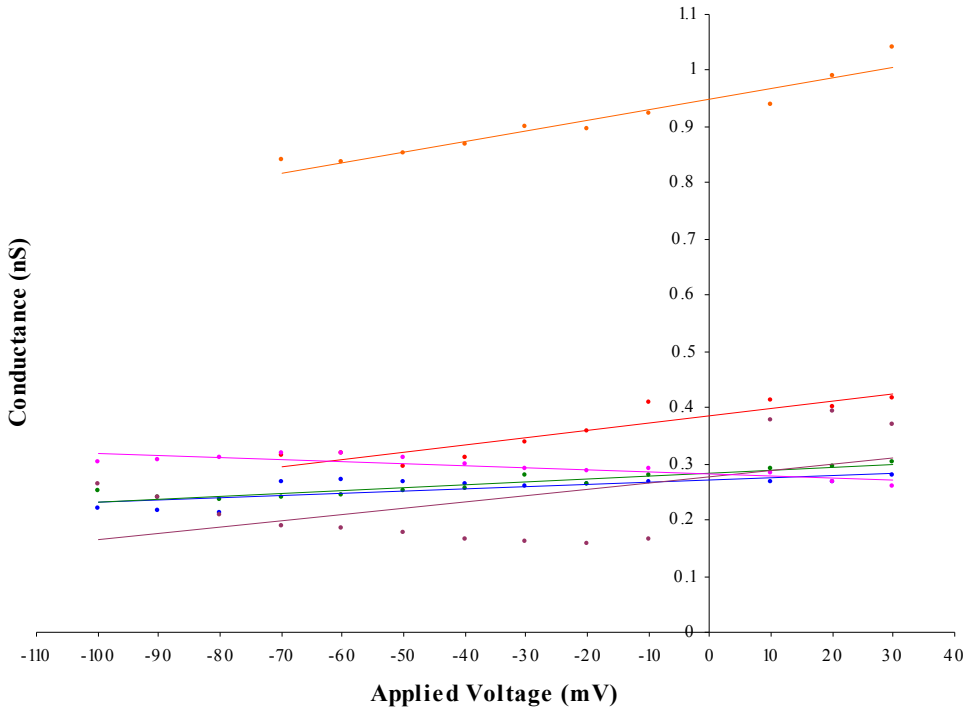

Fig. 22. Conductance Comparison for the Low B103 Subset. Mean values for control (blue), 10 μM 5-HT (green), 500 μM 5-HT (red), 1 mM 5-HT (orange), 5 μM d-tubocurarine (plum), and 5 μM d-tubocurarine plus 10 μM 5-HT (pink) are shown plotted against applied voltage. The solid lines represent the lines of best fit for each averaged data series. Clearly demonstrated is an increase in channel conductance associated with the addition of increasing concentrations of 5-HT so that 1 mM > 500 μM > 10 μM. Also shown is a decrease in conductance with the 5 μM d-tubocurarine at hyperpolarising potentials however stimulation with 5 μM d-tubocurarine and 10 μ M 5-HT at hyperpolarising potentials appears to increase the low subset conductance above that seen with 10 μM 5-HT alone. Further research will be required to isolate the cause of this increase.

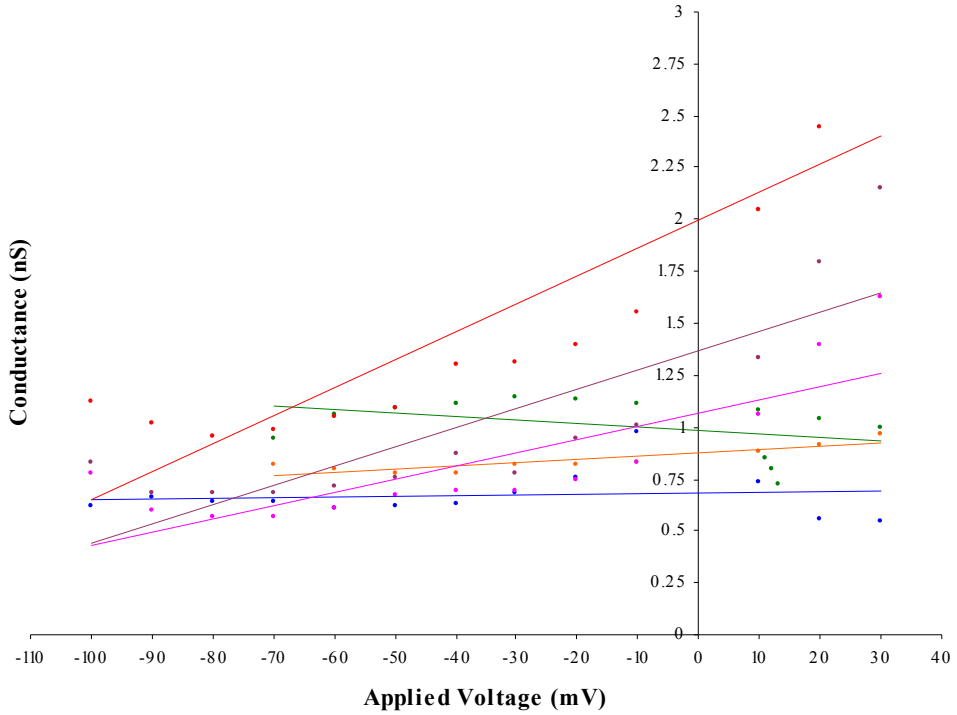

Fig. 23. Conductance Comparison for the Medium B103 Subset. Mean values for control (blue), 10 μM 5-HT (red), 500 μM 5-HT (green), 1 mM 5-HT (orange), 5 μM d-tubocurarine (plum), and 5 μM d-tubocurarine plus 10 μM 5-HT (pink) are shown plotted against applied voltage. The solid lines represent the lines of best fit for each averaged data series. Clearly demonstrated is a decrease in channel conductance associated with the addition of increasing concentrations of 5-HT so that 10 μM > 500 μM > 1 mM. Also shown is an apparently agonistic effect cause by the addition of 5 μM d-tubocurarine, interestingly the response to d-tubocurarine alone shows a greater conductance to that seen with 10 μM 5-HT as well. Further research will be required to isolate the cause of this phenomenon.

4. Discussion and conclusion

We describe the ionic movements in the physiological and symmetric solutions. The solutions used for physiological normal control results employed K^+ as the primary pipette solution cationic component, and Na^+ as the primary bath cation. This was because the normal conditions under which a cell exists demonstrates a higher internal K^+ than Na^+ concentration, thus recorded current results mimicked normal phenomenon. This meant that response currents were expected to be primarily carried mainly by K^+ efflux or Na^+ influx.

Ion movement is dependent on the electrochemical gradient produced only by its own subset of ions, thus it is independent of the concentration of other ions. This means that movement of Na^+ in solution is caused by the relative concentration of Na^+ alone and is not affected by the concentration of other ions in solution. In normal physiological conditions (*in*

vivo) early transient currents that reverse their signs from inward current flow to outward current flow at values greater than around -60 mV (normal membrane resting potential) would be expected to be carried by Na^+ so that correspondingly our experimental results in normal physiological solutions ought to be reversing at around -91.2 mV (E_{Na+}). Alternatively late outward currents would be expected to be carried by K^+ with a E_{rev} more negative than -60 mV. A comparison of E_{rev} for Na^+ (91.2 mV), K^+ (-78.3 mV), Ca^{2+} (0.007), and Cl^- (-0.05) with the recorded E_{rev} (0.14 mV) clearly indicated that currents were passing through the point of origin demonstrating non-selective ion permeation.

The single-channel current responses noted for cells in physiologically normal solutions indicated the probability of multiple channel subconductance states (Figure#21). With a maximum conductance of 0.95 pS and an average of 0.25 nS. The probable true maximum conductance state for the channel was when 13.30 pA of current was recorded (0.44 nS). Subconductance states exist because while a channel might be open, and therefore conducting ions, it might not be fully activated or conducting at its full capacity.

While the normal physiological ionic concentration of a cell's environment is not symmetrical (i.e. the intracellular fluid and extracellular fluid do not have the same ionic composition) current recordings of a particular selective channel can be enhanced by using symmetrical solutions with a greater than normal concentration of the specific permeant ion. Na^+ was used in this experimental series in order to emphasis and characterise the kinetics of known channels.

The B103 cells were divided into three electrophysiological response groups based on the observed variation in cellular current response to -100 mV stimulus in symmetrical bathing and pipette solutions: low, medium, and high conductance B103 subsets.

The averaged maximum conductance control result (0.28 pS at +30 mV) indicates that this subset shows its highest voltage-determined conductance at **positive potentials** (>0 mV) thus displaying **outward current rectification** (positive ions move from the cellular cytoplasm into the surrounding solution).

A fast-activating increase in channel conductance in response to the addition of serotonin was observed, where an increase in 5-HT concentration resulted in a higher conductance level, so that conductance response for the low B103 subset was 1 mM > 500 μM > 10 μM (Figure#22).

E_{rev} for the low subset varied from control -0.13 mV to 2.46 mV for 5μM d-tubocurarine. While most of the values fell close enough to E_{Na+} (0.0 0± 0.5 mV) to indicate that Na^+ was the primary ionic contributor to current the values for 500 μM and 1 mM 5-HT and 5 μM d-tubocurarine were slightly higher suggesting other ions produced some component of these conductances. Further experiments (where ions are selectively removed from the bath and pipette) are required to identify the percentage of current response comprised by components other than Na^+. Only a fraction of the delayed steady-state current response could have been caused by Ca^{2+} permeation, however, as very little Ca^{2+} was presenting the symetrical solutions. This low concentration was deliberately produced as in the normal cellular resting state cytoplasmic free Ca^{2+} levels are held at extremely low concentrations lying in the range of 20-300 nM in living cells. This concentration is maintained by the combined action of the ATP-dependent pump and Na^+/Ca^{2+} exchanger systems on the

surface of the membrane, as well as by ATP-dependent pumps present on intracellular organelles such as the endoplasmic reticulum.

In the low subset recordings (Figure#10) there was a high frequency response component to 10 μM 5-HT at -100 mV, just before the initiation of the steady-state current. This may indicate the 5-HT_3 receptor channel current component.

A heterogeneity of current responses was observed for 500 μM 5-HT applied to the medium subset demonstrating the presence of different receptor conductance states which keep on increasing even after 5000 ms. By 5000 ms the steady-state current amplitude get doubled as compared to the initial response. Receptor heterogeneity was again displayed in the presence of 1 mM 5-HT where some receptors were silent at hyperpolarising potentials while some were bursting. An increasing current after 5000 ms again indicated continued channel opening or increase in subconductance levels.

A comparison of the mean conductances recorded for the varying concentrations of 5-HT for medium B103 cells (Figure#23) shows that the cells demonstrated a decreasing current response to increasing 5-HT concentration where 10 μM > 500 μM > 1 mM. These results are comparable to the results previously obtained for N1E-115 cells, where maximal response was noted at 10 μM 5-HT (Neijt, Duits, & Vijverberg, 1988). Only 500 μM 5-HT stimulated the high subset of B103 cells, with the ±30 mV slope conductance showing that depolarising potentials demonstrate a higher conductance. Further investigation is warranted to clarify this decreased response.

D-tubocurarine was employed as a competitive antagonist to identify 5-HT_3Rs in B103 cell-lines. The recorded responses to d-tubocurarine indicated that rather than antagonising 5-HT_3R activity it was having a modulatory affect on the native B103 receptors for both low and medium subsets. The low cells had a more normal response with a decrease in conductance seen with d-tubocurarine at hyperpolarising potentials, however stimulation with both d-tubocurarine and 10 μM 5-HT at hyperpolarising potentials appeared to increase subset conductance to a level above that seen with 10 μM 5-HT alone.

Our results are indicative of either a change in the amino acid composition of the antagonist binding area of the 5-HT_3R (indicating different subunit composition of 5-HT_3R in these cell-lines as compared to native neuronal cells or isolated recombinant α and β subtypes), or that the same subunits are present with different amino acid compositions (splice variants). Also, at low concentrations some antagonist can act as positive modulators of receptors. Further research will be required to isolate the cause of this increase.

In summary, we describe the patch clamp experiments for B103 cells as **Black Box Test Known Inputs**

1. B103 cells were chosen for patching based on their general morphology: approximately 25 μm in diameter, well-defined clean cell membrane.
2. Only non-contaminated healthy B103 cells were used for patch clamp experiments.
3. Two sets of bath and pipette solutions were used through out the experiments. One which mimics the Extracellular and intracellular ionic composition and second with similar sodium concentration on both side of the cell membrane as to get close to zero reversal potential. The second set of solution was used to observe the serotonin gated currents.

4. Serotonin solutions of different known concentrations were used in the bath to see 5-HT3R currents. In these experiments TTX or phenytoin solution were used to abolish any endogenous currents
5. Pharmacological agents from the same companies were used through out the experiments.
6. Well-regulated bath perfusion system was used to challenge patched cells with serotonin hydrochloride solutions of 1 mM, 500 μM, and 10 μM concentrations.
7. Thin walled borosilicate glass capillaries (1.5 mm O.D. × 1.17 mm I.D) were used to produce patch pipettes with a 3 MΩ resistance. Pipettes were half-filled using both the front- and back-filling techniques
8. Same Patch clamp setup (HEKA EPC9 amplifier and HEKA *Pulse* software package) fully grounded without any noise was used through out the experiments, with daily calibration.
9. Constant Pulse Protocol facilitated via the HEKA *Pulse* software was used through out the experiments. Voltage procedure design for the voltage gated experiments ranges from -100 mV to +30 mV increasing in 10 mV steps with a resting period at 0 mV between each step.
10. B103 cells were categorized into three types based on their current response to the maximum hyperpolarizing step in the Protocol, which is at -100mV. Responses that were observed to be of 30 pA or less were categorized into low subset, between 30-100 pA were categorized into the medium subset and more than 100 pA in high subset.

Unknown outputs (some examples)

1. B103 cells with similar morphology and experimental conditions randomly generate three different sub sets of conductances.
2. An increasing steady state current even after 5000 ms in the medium subset
3. Only 500 μM 5-HT stimulated the high subset of B103 cells.
4. Action of d-tubocurarine as agonist to B103 currents of both low and medium subsets.
5. The low sub set cells had a more expected response with d-tubocurarine at hyperpolarising potentials.
6. D-tubocurarine in the presence of 10 μM 5-HT at hyperpolarising potentials increases 5-HT3 currents more than that seen with 10 μM 5-HT alone.

Looking for answers to the unknown outcomes and mechanisms of our experiments.

5. References

[1] Alien, D.H., Lepple-Wienhues, A., Cahalan, MD 1997. Ion channel phenotype of melanoma cell lines. J. Membr. Biol. 155:27–34

[2] Branchek T., Kates M., Gershon M.D. 1984. Enteric receptors for 5-hydroxytryptamine. *Brain Research.* 324(1):107-118.

[3] Dahlstrom A., Fuxe K. 1960. Evidence for the existence of monoamine-containing neurons in the central nervous system. I Demonstration of monoamines in the cell bodies of brain stem neurons. *Acta Physiologia Scandinava.* 62:1-55.

[4] Druckrey H., Preussmann R., Ivankovic S., Schmahl D. 1967. Organotropic carcinogenic effects of 65 various N-nitroso- compounds on BD rats. *Zeitschrift fur Krebsforschung.* 69(2):103-201

[5] Fraser, S.P., Diss, J.K.J., Mycielska, M.E., Coombes, R.C., Djamgoz, M.B.A 2002. Voltage-gated sodium channel expression in human breast cancer cells: Possible functional role in metastatis. Breast Cancer Research & Treatment 76 (Suppl 1):S142

[6] Freschi J.E., Shain W.G. 1982.Electrophysiological and pharmacological characteristics of the serotonin response on a vertebrate neuronal somatic cell hybrid. *The Journal of Neuroscience.* 2(1):106-112.

[7] Greenshaw A.J. 1993. Behavioural pharmacology of 5-HT3 receptor antagonists: a critical update on therapeutic potential. [Review]. *Trends in Pharmacological Sciences.* 14(7):265-270.

[8] Hales T.G., Tyndale R.F. 1994. Few cell lines with $GABA_A$ mRNAs have functional receptors. *Journal of Neuroscience.* 14(9):5429-5436.

[9] Hamil O. P., Marty A., Neher E.,Sakmann B., Sigworth F., 1981 Improved patch clamp techniques for high-resolution current recordings from cells and cell free membrane patches. Pfluger Archive. 391: 85-100

[10] Kasckow J.W., Tillakaratne N.J., Kim H., Strecker G.J., Tobin A.J., Olsen R.W. 1992. Expression of $GABA_A$ receptor polypeptides in clonal rat cell lines. *Brain Research.* 581(1):143-147.

[11] Kilpatrick G.J., Jones B.J., Tyers M.B. 1987. Identification and distribution of 5-HT3 receptors in rat brain using radioligand binding. *Nature.* 330 (6150):746-748.

[12] Kirk E.E., Giorano J., Anderson R.S. 1997. Serotonergic receptors as targets for pharmacotherapy. [Review]. *Journal of Neuroscience Nursing.* 29(3):191-197.

[13] Lambert J.J., Peters J.A., Hales T.G., Dempster J. 1989. The properties of 5-HT3 receptors in clonal cell lines studied by patch-clamp techniques. *British Journal of Pharmacology.* 97(1):27-40.

[14] Laniado, M.E., Lalani, E.N., Fraser, S.P., Grimes, J.A., Bhangal, G., Djamgoz, M.B.A., Abel, P.D 1997. Expression and functional analysis of voltage-activated Na+ channels in human prostate cancer cell lines and their contribution to invasion in vitro. Am. J. Pathol. 150:1213–1221

[15] Maricq A.V., Peterson A.S., Brake A.J., Myers R.M., Julius D. 1991. Primary structure and functional expression of the 5HT3 receptor, a serotonin-gated ion channel. *Science.* 254(5030):432-437.

[16] Mook-Jung I., Joo I., Sohn S., Kwon H.J., Huh K., Jung M.W. 1997. Estrogen blocks neurotoxic effects of beta-amyloid (1-42) and induces neurite extension on B103 cells. *Neuroscience Letters.* 235(3):101-104.

[17] Napias C., Olsen R.W., Schubert D. 1980. GABA and picrotoxinin receptors in clonal nerve cells. *Nature.* 283(5744):298-299.

[18] Neijt H.C., Te Duits I.J., Vijverberg H.P.M 1988. Pharmacological characterization of serotonin 5-HT3 receptor-mediated electrical response in cultured mouse neuroblastoma cells.. *Neuropharmacology.* 27(3):301-307.

[19] Ninomiya H., Roch J.M., Jin L.W., Saitoh T. 1994. Secreted form of amyloid beta/A4 protein precursor (APP) binds to two distinct APP binding sites on rat B103 neuron-like cells through two different domains, but only one site is involved in neuritotropic activity. *Journal of Neurochemistry.* 63 (2):495-500.

[20] Peters J.A., Lambert J.J. 1989. Electrophysiology of 5-HT3 receptors in neuronal cell lines. [Review]. *Trends in Pharmacological Sciences.* 10 (5):172-175.

[21] Roger, S., Besson, P., Le Guennec, J.Y 2003. Involvement of a novel fast inward sodium current in the invasion capacity of abreast cancer cell line. Biochim Biophys Acta. 1616:107–111

[22] Schubert D., Heinemann S., Carlisle W., Tarikas H., Kimes B., Patrick J., Steinbach J.H., Culp W., Brandt B.L. 1974. Clonal cell lines from the rat central nervous system. *Nature.* 249(454):224-227.

[23] Schubert D. 1975. The uptake of GABA by clonal nerve glia. *Brain Research.* 84(1):87-98.

[24] Segal M. M and Douglas, A. F. 1997. Late Sodium Channel Openings Underlying Epileptiform Activity Are Preferentially Diminished by the Anticonvulsant Phenytoin *J Neurophysiol* 77: 3021-3034

[25] Tyndale R.F., Hales T.G., Olsen R.W., Tobin A.J. 1994. Distinctive patterns of GABAA receptor subunit mRNAs in 13 cell lines. *Journal of Neuroscience.* 14(9):5417-5428.

[26] Wallis D.I., Woodward B. 1975. Membrane potential changes induced by 5-hydroxytryptamine in the rabbit superior cervical ganglion. *British Journal of Pharmacology. 55*(2):199-212.

[27] Yan D., Schulte M.K., Bloom K.E., White M.M. 1999. Structural features of the ligand-binding domain of the serotonin 5HT3 receptor. *Journal of Biological Chemistry.* 274(9):5537-5541.

[28] Yoshifumi Kawanabe , Nobuo Hashimoto, Tomoh Masaki 2001 B103 neuroblastoma cells predominantly express endothelin ET_B receptor; effects of extracellular Ca^{2+} influx on endothelin-1-induced mitogenesis Eur J of Pharmacol 425 (3), 173-179

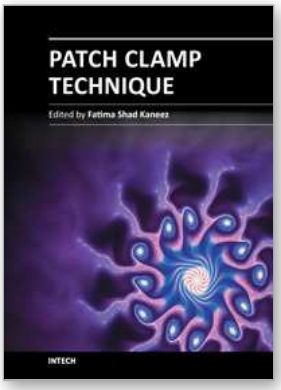

Patch Clamp Technique

Edited by Prof. Fatima Shad Kaneez

ISBN 978-953-51-0406-3
Hard cover, 356 pages
Publisher InTech
Published online 23, March, 2012
Published in print edition March, 2012

This book is a stimulating and interesting addition to the collected works on Patch clamp technique. Patch Clamping is an electrophysiological technique, which measures the electric current generated by a living cell, due to the movement of ions through the protein channels present in the cell membrane. The technique was developed by two German scientists, Erwin Neher and Bert Sakmann, who received the Nobel Prize in 1991 in Physiology for this innovative work. Patch clamp technique is used for measuring drug effect against a series of diseases and to find out the mechanism of diseases in animals and plants. It is also most useful in finding out the structure function activities of compounds and drugs, and most leading pharmaceutical companies used this technique for their drugs before bringing them for clinical trial. This book deals with the understanding of endogenous mechanisms of cells and their receptors as well as advantages of using this technique. It covers the basic principles and preparation types and also deals with the latest developments in the traditional patch clamp technique. Some chapters in this book take the technique to a next level of modulation and novel approach. This book will be of good value for students of physiology, neuroscience, cell biology and biophysics.

How to reference

In order to correctly reference this scholarly work, feel free to copy and paste the following:

K. Fatima-Shad and K. Bradley (2012). Patch ClampTechnique for Looking at Serotonin Receptors in B103 Cell Lines: A Black Box Test, Patch Clamp Technique, Prof. Fatima Shad Kaneez (Ed.), ISBN: 978-953-51-0406-3, InTech, Available from: http://www.intechopen.com/books/patch-clamp-technique/patch-clamptechnique-for-looking-at-serotonin-receptors-in-b103-cell-lines-a-black-box-test

InTech Europe
University Campus STeP Ri
Slavka Krautzeka 83/A
51000 Rijeka, Croatia
Phone: +385 (51) 770 447
Fax: +385 (51) 686 166
www.intechopen.com

InTech China
Unit 405, Office Block, Hotel Equatorial Shanghai
No.65, Yan An Road (West), Shanghai, 200040, China
中国上海市延安西路65号上海国际贵都大饭店办公楼405单元
Phone: +86-21-62489820
Fax: +86-21-62489821